Sexually dimorphic metabolism of branched-chain lipids in C57BL/6J mice

Barbara P. Atshaves,* **H. Ross Payne,**[†] **Avery L. McIntosh,*** **Shane E. Tichy,**[§] **David Russell,**[§] **Ann B. Kier,**[†] **and Friedhelm Schroeder**[1,*,§]

Departments of Physiology and Pharmacology,* Pathobiology,[†] and Chemistry,[§] Texas A&M University, College Station, TX 77843-4466

Abstract Despite the importance of branched chain lipid oxidation in detoxification, almost nothing is known regarding factors regulating peroxisomal uptake, targeting, and metabolism. One peroxisomal protein, sterol carrier protein-x (SCP-x), is thought to catalyze a key thiolytic step in branched chain lipid oxidation. When mice with substantially lower hepatic levels of SCP-x were tested for susceptibility to dietary stress with phytol (a phytanic acid precursor and peroxisome proliferator), livers of phytol-fed female but not male mice *i*) accumulated phytol metabolites (phytanic acid, pristanic acid, and Δ-2,3-pristanic acid); *ii*) exhibited decreased fat tissue mass and increased liver mass/body mass; *iii*) displayed signs of histopathological lesions in the liver; and *iv*) demonstrated significant alterations in hepatic lipid distributions. Moreover, both male and female mice exhibited phytol-induced peroxisomal proliferation, as demonstrated by liver morphology and upregulation of the peroxisomal protein catalase. In addition, levels of liver fatty acid binding protein, along with SCP-2 and SCP-x, increased, suggesting upregulation mediated by phytanic acid, a known ligand agonist of the peroxisomal proliferator-activated receptor α. In summary, the present work establishes a role for SCP-x in branched chain lipid catabolism and demonstrates a sexual dimorphic response to phytol, a precursor of phytanic acid, in lipid parameters and hepatotoxicity.—Atshaves, B. P., H. R. Payne, A. L. McIntosh, S. E. Tichy, D. Russell, A. B. Kier, and F. Schroeder. Sexually dimorphic metabolism of branched-chain lipids in C57BL/6J mice. *J. Lipid Res.* 2004. **45:** 812–830.

Supplementary key words sterol carrier protein-2 • sterol carrier protein-x • liver fatty acid binding protein • peroxisome proliferator-activated receptor α • peroxisome • phytanic acid • hepatocellular toxicity • sexual dimorphism

Mammals absorb substantial amounts of branched-chain lipids from their diets, including phytol (1, 2) and cholesterol (3–7). Phytol, a dietary branched-chain lipid alcohol derived by ruminant bacterial cleavage of the side chain of chlorophyll, is converted to phytanic acid in the gut. A variety of peroxisomal disorders involve the inability to oxidize branched-chain fatty acids and result in increased levels of phytanic acid, which can lead to toxicity (8, 9). Thus, it is essential that excess branched-chain lipids be oxidized to prevent hepatocellular toxicity. In mammals, phytol is sequentially metabolized in a series of enzymatic steps occurring first outside peroxisomes, where oxidation of phytol to phytanic acid and conversion to phytanoyl-CoA occurs, followed by transport of phytanoyl-CoA into peroxisomes (10, 11). Within the peroxisome, the phytanoyl-CoA undergoes several cycles of α-oxidation followed by β-oxidation to sequentially form pristanic acid, pristanoyl-CoA, Δ-2,3-pristenoyl-CoA, 3-OH-pristanoyl-CoA, 3-ketopristanoyl-CoA, and 4,8,12-trimethyltridecanoyl-CoA [reviewed in ref. (12)]. Completion of the metabolism of shortened products occurs after transport out of the peroxisome and to mitochondria for additional oxidative steps [reviewed in ref. (12)]. Thus, peroxisomal oxidation is essential for the metabolism of branched-chain lipids (phytol) to prevent the accumulation of potentially toxic compounds. However, although experiments performed in vitro as well as correlative studies suggest that several proteins, including the sterol carrier protein-2 (SCP-2) family of proteins (SCP-x and SCP-2), may participate in these important metabolic steps, little is known regarding factors that regulate either the cell uptake and/or the intracellular targeting of branched-chain fatty acids to peroxisomes.

For several decades, the main role of SCP-x and SCP-2 has been thought to be involvement in intracellular

Abbreviations: CCD, charge coupled device; DAB, 3,3′-diamino-benzidine; DEXA, dual-energy X-ray absorptiometry; FAME, fatty acid methyl ester; FAT, fatty acid translocase; L-FABP, liver fatty acid binding protein; PAS, periodic acid-Schiff; PPAR, peroxisome proliferator-activated receptor; SCP-2, sterol carrier protein-2; SCP-x, sterol carrier protein-x; TEM, transmission electron microscopy.

[1] To whom correspondence should be addressed.
e-mail: fschroeder@cvm.tamu.edu

cholesterol transport. Although the full physiological function of both proteins remains to be resolved, recent developments in molecular and cell biology identified additional interrelationships between these ubiquitous proteins and suggested new physiological role(s) in branched-chain lipid oxidation [reviewed in refs. (13–15)]. Studies with the SCP-x protein indicate that along with its inherent ability to transport lipids such as cholesterol (16), this protein has unique roles in the peroxisomal β-oxidation of branched-chain fatty acids and in bile acid formation from cholesterol (17–20). Although in vitro experiments show that SCP-x has the same substrate specificity for straight-chain fatty acids as that of the conventional peroxisomal thiolases, SCP-x also has a unique ability to catalyze the thiolytic cleavage of 3-oxoacyl-CoA esters of branched-chain molecules with methyl groups at the 2-position, such as pristanic acid (17, 19, 21) and cholestanoic acid (22).

Unlike SCP-x, SCP-2 has no enzymatic activity. However, studies performed in vitro and with cultured cells indicate that SCP-2 binds a variety of lipids (fatty acid, fatty acyl-CoA, cholesterol, phospholipid) (23–25), transports the respective bound ligands, targets the ligands to specific intracellular sites, and enhances the metabolism of the ligands [reviewed in ref. (13)]. Studies with intact cells overexpressing SCP-2 show that SCP-2 accelerates the intracellular transfer of fatty acids (26, 27). The responses of both SCP-x and SCP-2 overexpression to supplementation with phytanic acid was shown to be highly dose dependent: i) at low phytanic acid levels, SCP-x and SCP-2 stimulate phytanic acid oxidation severalfold more than that of straight-chain fatty acids (SCP-x >> SCP-2), with concomitant enhancement of the esterification of both branched- and straight-chain fatty acids (28); ii) at high phytanic acid levels, phytanic acid oxidation is inhibited (SCP-x >> SCP-2) and cells exhibit signs of toxicity (29). Both SCP-x and SCP-2 contain a peroxisomal targeting signal at the C terminus, suggesting peroxisomal localization [reviewed in ref. (13)]. However, although SCP-x is almost exclusively peroxisomal, a variety of studies (copurification with peroxisomal catalase, immunogold electron microscopy, and immunofluorescence) reveal that as much as half of total SCP-2 is extraperoxisomal [reviewed in ref. (13)]. Thus, SCP-2 is ideally localized to serve in the transport of fatty acids and/or their fatty acyl-CoA derivatives to and within peroxisomes (where branched-chain fatty acid and cholestanoic acid oxidation are initiated) (9).

In summary, the studies cited above suggest a strong correlation for SCP-x and SCP-2 in fatty acid metabolism, particularly in peroxisomal oxidation. However, the individual physiological functions of these proteins in branched-chain lipid oxidation have not been definitively resolved in vivo. To begin to resolve these issues, the present biochemical and morphological investigation took advantage of the intrinsically low level of SCP-x in female versus male mice (30) to examine peroxisomal phytanic acid metabolism and fat accumulation in response to dietary phytol.

MATERIALS AND METHODS

Materials

Silica gel G and Silica gel 60 thin layer chromatography plates were from Analtech (Newark, DE) and EM Industries, Inc. (Darmstadt, Germany), respectively. Neutral lipid and fatty acid standards were purchased from Nu-Chek Prep, Inc. (Elysian, MN), whereas phospholipid standards were obtained from Avanti (Alabaster, AL). Phytanic acid was purchased from Sigma (St. Louis, MO). Rabbit polyclonal antisera to recombinant human SCP-2, mouse SCP-x, and rat liver fatty acid binding protein (L-FABP) were prepared as described previously (31). Sheep anti-bovine catalase was purchased from Biodesign (Kennebunk, ME). Antiserum against CD-36 [also called fatty acid translocase (FAT)] was purchased from Research Diagnostics (Flanders, NJ). Rabbit polyclonal anti-human peroxisome proliferator-activated receptor α (PPARα) was purchased from Santa Cruz Biotechnology (Santa Cruz, CA). All reagents and solvents used were of the highest grade available and were cell culture tested.

Animal studies

Adult male and female (2 months of age, 20–30 g) inbred C57BL/6J mice were obtained from the Frederick Cancer Research and Development Center (Frederick, MD) and maintained on a standard rodent chow mix (5% calories from fat). Mice were given free access to food and water and were kept on a constant light cycle of 12 h of light/12 h of dark. Mice in the facility are monitored quarterly for infectious diseases and are specific pathogen free, particularly in reference to mouse hepatitis virus. Animal protocols were approved by the Animal Care and Use Committee of Texas A&M University.

One week before the start of experiments, male and female mice were switched to a modified AIN-76A rodent diet (5% calories from fat; diet D11243; Research Diets, Inc., New Brunswick, NJ). The modified AIN-76A rodent diet (control diet) was chosen because it is essentially phytoestrogen free (32, 33). Because phytoestrogens are known to exert estrogenic effects in mice, this avoids potential secondary complications in gender comparisons (32, 33). After 1 week, the male and female mice were each divided into three groups (six mice/group): group 1 remained on the control diet; group 2 was switched to a modified AIN-76A rodent diet supplemented with 0.5% phytol (5% calories from fat; diet D01020601; Research Diets, Inc.); group 3 was transferred to a modified AIN-76A rodent diet supplemented with 0.2% clofibric acid (5% calories from fat; diet D01020602; Research Diets, Inc.).

The effects of phytol on both male and female mice were examined because previous feeding studies were performed only on male mice; thus, the effect of phytol on female mice (with 5-fold lower levels of SCP-x) was not reported (1, 12, 34). The 0.5% phytol level was chosen because earlier work showed that feeding higher phytol levels (2–5%) resulted in extensive liver toxicity and animal mortality, whereas lower levels (0.05%) showed minimal effects (1). Therefore, the 0.5% phytol level was chosen to promote limited toxicity, weight loss, and accumulation of phytol metabolites over several weeks without the added effects of extreme toxicity leading to premature death. To equate the amounts of phytol consumed daily by the mice in the 0.5% feeding study with amounts typically consumed daily by humans, the following estimations were made. In humans, daily dietary intake of phytol and its metabolite phytanic acid is on the order of 50–100 mg/day (2, 9). The phytol-fed mice ingested ∼250 mg of phytol per day on the 0.5% phytol diet. In terms of milligrams of phytol per gram of body weight, the mice ingested 10 mg/g/day, whereas an average value for human consumption would be

0.0014 mg/g/day for a 70 kg man. Although dairy products such as butter, margarine, and cheeses can contain up to 500 mg phytanic acid/100 g wet weight, with lower amounts reported in milk, veal, codfish, beef liver, and egg yolks (2), it becomes clear that substantial amounts would need to be ingested to reach levels equivalent to those consumed in the 0.5% phytol feeding study (700 g/70 kg/day for human consumption). Although phytol toxicity is not normally a problem with healthy individuals, it becomes an issue when peroxisomal disorders (Refsum's disease) result in an inability to metabolize phytol (2, 9).

Body weight and food intake were monitored every other day. At the end of the study (day 19), animals were fasted overnight and anesthetized (100 mg/kg ketamine, 10 mg/kg zylaxine), and blood was collected by cardiac puncture followed by cervical dislocation to ensure humane death. Percentage total body fat, fat tissue mass, and lean tissue mass were determined by dual-energy X-ray absorptiometry (DEXA) using a Lunar PIXImus densitometer (Lunar Corp., Madison, WI). Briefly, in vivo determination of body composition was performed by exposing the entire animal to sequential beams of high- and low-energy X-rays with an image taken of the X-rays hitting a luminescent panel. Measurement of the ratios of attenuation at the different energies allows the separation of bone mass from tissue samples. Tissue mass was further separated into lean and fat tissue mass to give accurate values of body composition. Calibration was performed with a phantom mouse of known bone mineral density and fat tissue mass, followed by correlation to chemical extraction techniques (35).

Livers were harvested and weighed, and several from each feeding group were immediately photographed with a pixel resolution of 2,048 × 1,536 using an Olympus C-3030 Zoom digital camera (Olympus America, Inc., Melville, NY) equipped with an appropriate zoom adaptor and macro lens. To uniformly illuminate the livers, a ring light was constructed in the laboratory of white light-emitting diodes (RadioShack Corp., Fort Worth, TX). This light was mounted between the macro lens and the camera, which was rigidly attached to a laboratory ring stand. Images were processed using Corel Photo-Paint 9 (Corel Corp., Ottawa, Ontario, Canada). Slices of liver were trimmed for electron microscopy and histological examination. Remaining portions of liver were snap-frozen on dry ice and stored at −80°C for lipid and Western analyses.

Pathology and light microscopy

After livers and other tissues were examined grossly, liver slices were excised near the *porta hepatis*, fixed in 10% neutral buffered formalin for 24 h, and stored in 70% alcohol until processed and embedded in paraffin. Paraffin-embedded sections were cut at 4–6 m thickness and stained with hematoxylin and eosin for overall histological evaluation, and other sections were stained with periodic acid-Schiff (PAS) for histochemistry of glycogen distribution. Similarly obtained liver slices were frozen in Tissue-Tek O.C.T. compound (Miles, Inc., Elkhart, IN) and stored at 20°C. Sections were cut at 4–6 m thickness and stained with oil red O for lipid evaluation.

Electron microscopy and image analyses

Small samples of liver (1–2 mm^3 segments) excised near the *porta hepatis* were fixed by immersion in glutaraldehyde and formaldehyde at room temperature. The peroxisomes in the liver cells were stained selectively for catalase by incubation in a reaction mixture containing 11 mM 3,3′-diaminobenzidine (DAB) in 0.1 M glycine buffer at pH 10.5 and 0.15% H_2O_2 for 1 h at 37°C. The tissue segments were postfixed in 2% OsO_4 in 0.1 M $NaPO_4$ buffer for 1 h, dehydrated in a graded alcohol series, and embedded in Spurr's epoxy resin. Semithin sections,

0.4 μm thick, were cut with a glass knife for the evaluation of DAB staining. Ultrathin sections of cells that contained DAB-stained peroxisomes were cut with a diamond knife, poststained lightly with uranyl acetate and lead citrate, and then examined and photographed with a Zeiss 10C electron microscope. Peroxisomal volume density (percentage of peroxisomal volume per total liver volume) was determined by morphometric analysis of 0.4 μm semithin sections of DAB-stained samples. Fifteen fields from each experimental group were acquired with an Olympus Vanox-S light microscope with an oil-immersion 100× objective lens and analyzed using the public domain ImageJ program (developed at the U.S. National Institutes of Health and available on the Internet at http://rsb.info.nih.gov/ij/). The image fields were randomly selected near the periphery of each liver sample from a 200 μm wide band of tissue that had the most uniformly and intensely stained peroxisomes. Areas of the liver not uniformly stained with DAB were excluded.

For morphometric measurements of lipid volume, fat droplets in the liver tissues were stained by a histological procedure described previously (36), with slight modifications. Briefly, formalin-fixed liver tissue was incubated for 8 h in 1% osmium tetroxide and 2.5% potassium dichromate, dehydrated in a graded ethanol series, and embedded in Unicryl resin. Semithin sections, 0.75 μm thick, were mounted on glass slides, coverslipped, and examined without counterstaining. These liver sections with darkly stained lipid droplets were imaged with a 40× light microscope objective and recorded with a Spot RT Slider cooled charge coupled device (CCD) camera. Four representative images were randomly selected from each liver for a total image area of 1 mm^2 per treatment group. The program ImageJ was used to determine the relative volume density of lipid droplets by measuring the image area occupied by the darkly stained lipid droplets as a fraction of the total image field of liver tissue. The area fraction determined by this method is an unbiased estimate of the volume fraction and is referred to as the relative volume density because the values were not corrected for the section thickness and did not exclude sinusoidal volume or nonparenchymal cells from the liver image (37).

Western blotting

Liver samples were homogenized (38) followed by centrifugation at 100,000 *g* for 1 h to isolate the soluble (cytosolic) fraction. Western blot analyses were performed to determine protein expression levels of catalase, L-FABP, SCP-2, SCP-x, and PPARα. Briefly, the cytosolic fractions (1–10 μg) were run on Tricine gels (12%) before transferring to 0.45 μm nitrocellulose paper (Sigma) by electroblotting in a continuous buffer system at 0.8 mA/cm^2 for 2 h. After transfer, blots were treated as described previously (31) using affinity-purified antisera against catalase, L-FABP, SCP-2, SCP-x, and PPARα. The extent of peroxisomal proliferation was determined by quantitation of catalase levels in the liver samples by Western analyses and by transmission electron microscopy (TEM) as described above. Proteins were quantified by densitometric analysis after image acquisition using a single-chip CCD video camera and a computer workstation (IS-500 system; Alpha Innotech, San Leandro, CA). Image files were analyzed (mean eight-bit grayscale density) using NIH Image (available by anonymous FTP).

Lipid analyses

Lipids were extracted from liver homogenates and serum (38) with *n*-hexane-2-propanol (3:2, v/v) (39, 40) and divided into portions for mass and fatty acid composition determination. One half of each extracted lipid sample was resolved into individual lipid classes and identified by comparison with known standards using Silica gel G thin-layer chromatography plates developed in

petroleum ether-diethyl ether-methanol-acetic acid (90:7:2:0.5) (39, 40). Total cholesterol, free fatty acid, triacylglyceride, cholesteryl ester, and phospholipid content were determined by the method of Marzo et al. (41). Protein concentration was determined by the method of Bradford (42) from the dried protein extract residue digested overnight in 0.2 M KOH. Lipids were stored under an atmosphere of N_2 to limit oxidation. All glassware was washed with sulfuric acid-chromate before use.

Transesterification

Acid-catalyzed transesterification was performed on the remaining half of the extracted lipid fraction from each sample to convert the lipid acyl chains to fatty acid methyl esters (FAMEs). FAMEs were then further extracted into *n*-hexane and separated by gas-liquid chromatography on a GLC-14A system (Shimadzu, Kyoto, Japan) equipped with a RTX-2330 capillary column (0.32 mm inner diameter × 30 m length; Restek, Bellefonte, PA). The injector and detector temperatures were set at 260°C, with a temperature program of 100°C for 1 min, 10°C/min to 140°C, 2°C/min to 220°C, hold for 1 min, then ramp at 10°C/min to 260°C. A Waters SAT/IN analytical-to-digital interface was used to collect peak area data and was converted to peak area using Millenium[32] 3.2 software. With the exception of phytanic acid metabolites, individual peaks were identified by comparison with known FAME standards (Nu-Chek Prep, Inc.) and referenced against a set concentration of 15:0 added before analysis.

Mass spectrometry

To further identify phytanic acid and its metabolites, mass spectra were acquired on an MDS Sciex (Concord, Ontario, Canada) API Qstar mass spectrometer using an Ionwerks (Houston, TX) time-to-digital converter, TDCx4, for data recording at 625 ps resolution. Samples were electrosprayed in the negative ion mode from a 1:1 solution of methanol-dichloromethane with an analyte concentration of 10 μM using the thermospray source. The spray voltage was maintained at −4,500 V. The nozzle-skimmer potential was set to −5 V to minimize fragmentation, and time-of-flight voltages were tuned to optimize the resolving power for the $[M-H]^-$ of phytanic acid (*m/z* 311) and pristanic acid (*m/z* 287). The following parameters were used: grid, +339 V; plate, −360 V; mirror, −960 V; and liner, −4,000 V. Acquisition and data analysis, including centroid measurements and resolving power calculations, were performed in TOFMA 2.0RC3.

Serum analyses

Collected blood samples were allowed to sit overnight at 4°C followed by centrifugation at 14,000 rpm for 20 min at 4°C, and the serum fraction was removed. Serum was analyzed for lipids as described above for liver lipids.

Statistics

Each feeding group consisted of five to six animals. All values are expressed as means ± SEM with n and *P* indicated in Results. Statistical analysis was performed using ANOVA combined with the Newman-Keuls multiple comparisons test (GraphPad Prism, San Diego, CA). Values with $P < 0.05$ were considered statistically significant.

RESULTS

Effect of branched-chain lipid (phytol) diet on body weight, food intake, and body composition of male and female C57BL/6J mice

A sexually dimorphic response to phytol treatment was established in male and female C57BL/6J mice when stan-
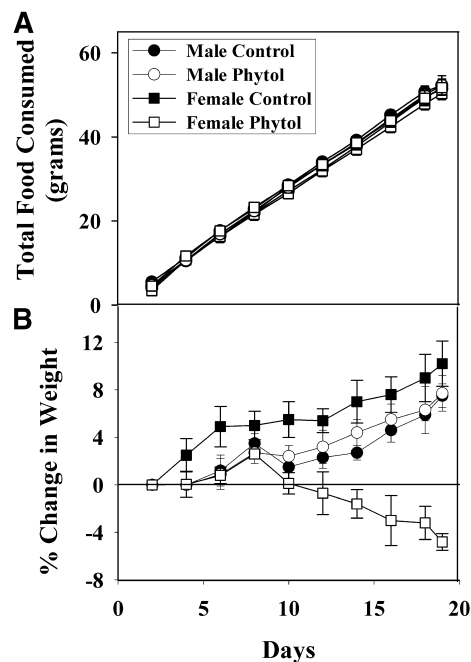

Fig. 1. Total food consumption and percentage change in weight of C57BL/6J male and female mice fed a defined diet with or without 0.5% phytol. The total amount of food consumed (A) and percentage change in body weight (B) were measured in male (circles) and female (squares) mice on control (closed symbols) and phytol (open symbols) diets. Values represent means ± SEM (n = 5–6).

dard chow was supplemented with 0.5% phytol for 19 days. Although food consumption was similar between the diet groups (**Fig. 1A**), male and female mice on control food and male mice on the phytol diet continued to gain weight during the feeding study. In contrast, female mice fed phytol lost weight and showed increased signs of toxicity (ruffled coat, less activity) after 10 days on the diet (Fig. 1B). Quantitation of the fat tissue mass and lean tissue mass by DEXA revealed that control females had 37% and 12% lower fat tissue mass (**Fig. 2C**) and lean tissue mass (Fig. 2D), respectively, compared with control males. Expressed as percentages, these data showed that the female mice gained significantly less of their weight as fat tissue mass (27% vs. 45%, respectively) compared with male mice (data not shown).

Although control-fed female mice gained weight over the entire 19 day feeding period, after 10 days the phytol-fed females began to lose weight (Fig. 1B, open squares vs. closed squares), were noticeably smaller (Fig. 2B), and showed increasing clinical signs of toxicity (ruffled coat, less activity). By 19 days on the phytol diet, female mice lost weight such that the average percentage change in weight (Fig. 1B, open squares vs. closed squares) was significantly lower by 12.9% compared with control-fed females ($P < 0.01$, n = 5–6). Representative DEXA images showed that phytol-fed females exhibited significantly decreased fat and lean tissue mass compared with control-fed female mice (Fig. 2C, D; $P < 0.05$, n = 5–6). In contrast, when phytol-fed male mice were compared with male mice on the control diet, similar increases in weight
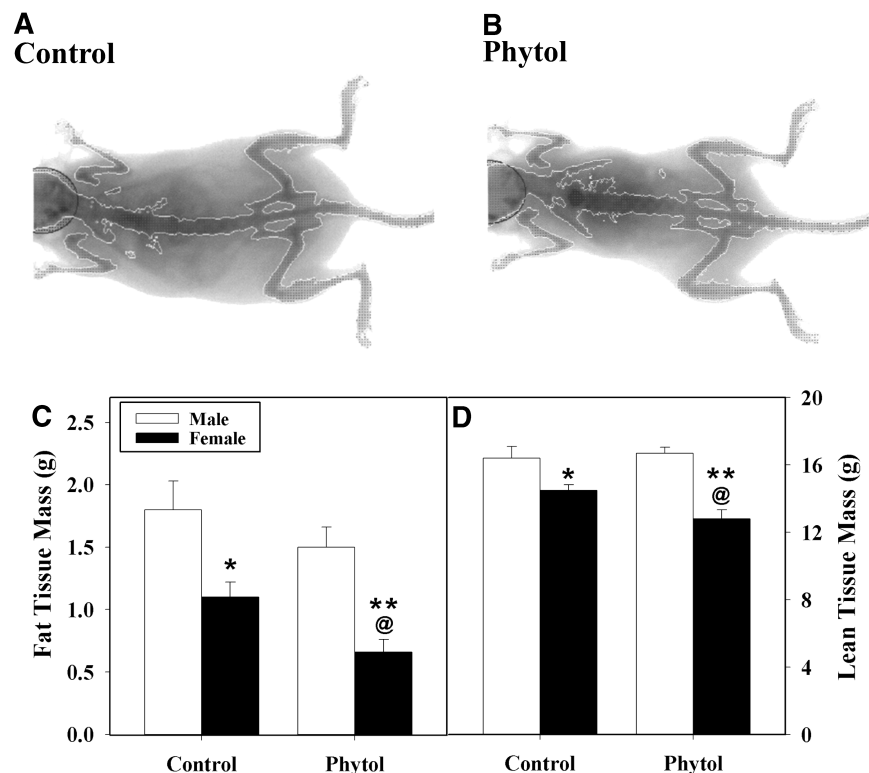
Fig. 2. Distribution of fat and lean tissue mass. Lunar PIXImus dual-energy X-ray absorptiometry scans of female C57BL/6J mice on control (A) and phytol (B) diets. Fat tissue mass (C) and lean tissue mass (D) were determined as described in Methods. Values represent means $\pm$ SEM. * $P < 0.05$ (n = 5–6) compared with males on the control diet. ** $P < 0.001$ (n = 5–6) compared with males on the phytol diet. @ $P < 0.05$ (n = 5–6) compared with females on the control diet.

gain were observed (Fig. 1B, open circles vs. closed circles). In addition, when analyzed by DEXA, phytol-fed males did not differ from control-fed males in terms of fat tissue mass (Fig. 2C) or lean tissue mass (Fig. 2D). Thus, phytol feeding did not alter body weight gain, the proportion of body fat, or the proportion of body lean tissue in male mice.

In summary, control-fed female and male mice consumed food and gained weight at similar rates. Females on the phytol diet lost weight (after 10 days) despite ingesting similar amounts of food, whereas phytol-fed males continued to gain weight. Thus, although phytol-fed males and females consumed the same calories, by 19 days the females actually lost weight compared with phytol-fed males or control-fed females. The weight loss in phytol-fed females (not seen in males) was preferentially in fat tissue mass (3-fold) versus lean tissue mass. These results suggested a sex-related difference in the ability to metabolize branched-chain fatty acids.

Effect of phytol on liver

Control male and female mice did not significantly exhibit different liver weights (**Fig. 3A**), liver weight-body weight ratios (Fig. 3B), or liver protein-liver weight ratios (Fig. 3C). However, males and females differed significantly in liver parameters in response to phytol diets.

Phytol-fed male mice showed gross enlargement of the liver, as indicated by a 27% increase in liver weight over male mice fed control food (Fig. 3A; $P < 0.01$, n = 5–6). Although the proportion of liver to body weight was unaltered by phytol feeding (Fig. 3B), phytol-fed males showed a 45% increase in liver protein-liver weight ratio, consistent with phytol-induced peroxisomal proliferation of liver proteins (Fig. 3C; $P < 0.001$, n = 5–6). Livers from male mice on the phytol or control diet appeared grossly normal (data not shown).

Phytol-fed female mice showed even greater gross morphological change in liver compared with control-fed females. The liver weight of phytol-fed female mice was 55% greater than for females on the control diet and 18% higher than for phytol-fed males (Fig. 3A; $P < 0.05$, n = 5–6). The proportion of liver to body weight was increased in female phytol-fed mice by 74% and 56% compared with female mice on the control diet and male mice on the phytol diet, respectively (Fig. 3B; $P < 0.05$, n = 5–6). However, phytol-fed females had similar liver protein-liver weight ratios as those on the control food (Fig. 3C), suggestive of liver enlargement attributable to fatty change, edema, and/or necrosis rather than from peroxisomal proliferation. Grossly, livers from female mice on phytol were consistently pale and friable and had a generalized mottled appearance (**Fig. 4B**). Livers from control-fed females appeared grossly normal (Fig. 4A). Livers
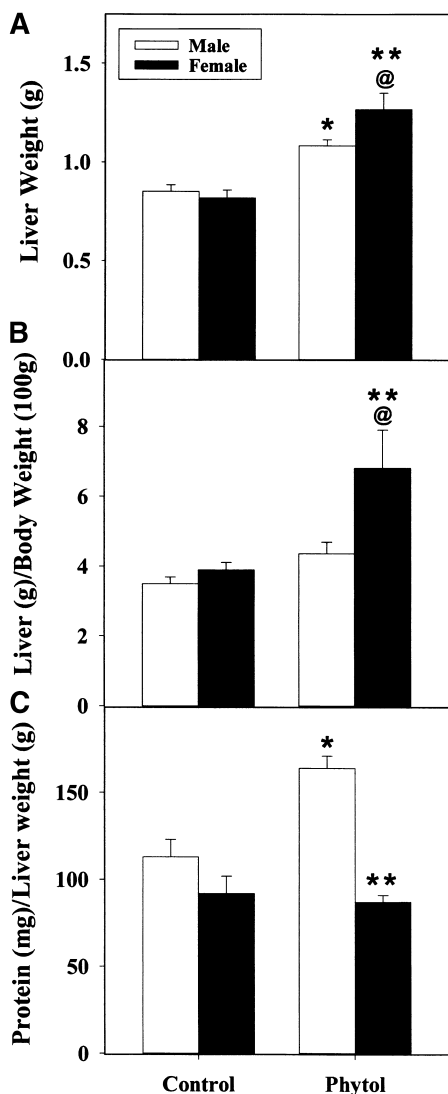
Fig. 3. Liver weight and protein content in mice. Liver weight (A), liver weight-body weight ratio (B), and protein weight-liver weight ratio (C) were determined in male and female mice fed control and phytol diets. Values represent means ± SEM. * $P < 0.001$ (n = 5–6) compared with males on the control diet. ** $P < 0.05$ (n = 5–6) compared with males on the phytol diet. @ $P < 0.05$ (n = 5–6) compared with females on the control diet.

from male mice on both the control and phytol diets appeared grossly normal (data not shown).

Histopathology

Marked histopathological lesions were present in phytol-fed female (**Fig. 5B–D**) but not in control-fed female (Fig. 5A), control-fed male (Fig. 5E), and phytol-fed male (Fig. 5F) mice. In female phytol-fed livers, random hepatic cords were disrupted and small multifocal areas of hepatocyte necrosis with early inflammatory cell infiltration of neutrophils and lymphocytes (microgranulomas) were observed (Fig. 5B). Isolated single-cell necrosis and possibly apoptosis of hepatocytes were located in these areas. Hepatocytes, particularly in midzonal regions, were both hypertrophic and hyperplastic. Hypertrophy was ex-
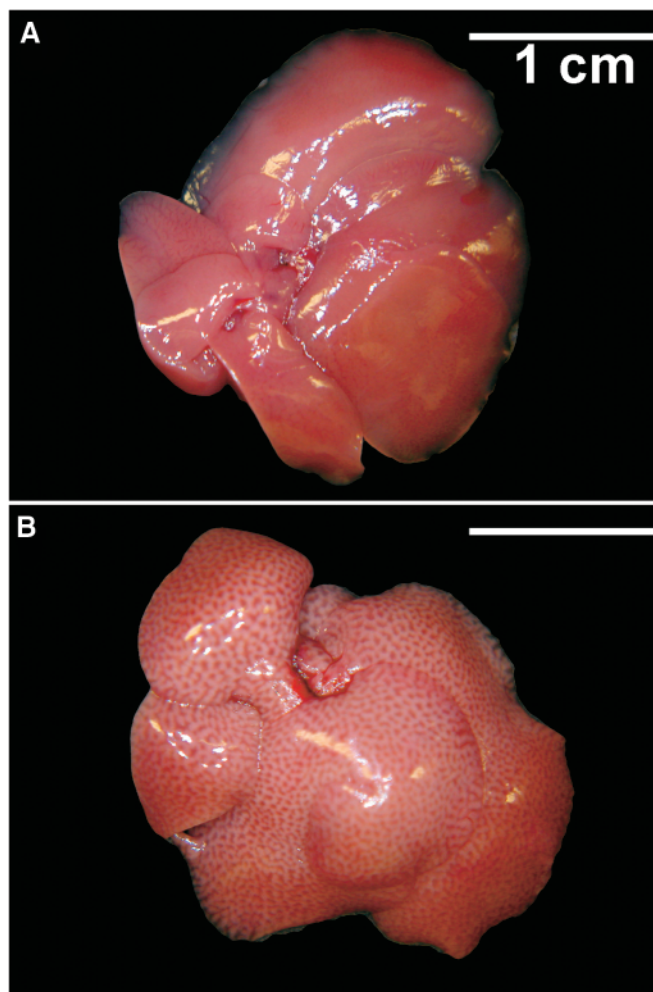

Fig. 4. Gross liver morphology. Livers from female C57BL/6J mice fed control and phytol diets were compared. A homogeneous red-brown color and normal size are seen in the control-fed mouse (A) versus an enlarged liver with paleness and mottling in the phytol-fed mouse (B).

hibited by hepatomegaly, with hepatocytes nearly 1.5–2 times normal size (Fig. 5C, D), and nuclear diploidy was increased. Hyperplasia was indicated by a significantly increased number of cells in mitosis and hepatocytoplasmic eosinophilia (Fig. 5D). Bizarre shapes of these mitotic figures were evident in cytomegalic cells (Fig. 5B–D), as if the cells were experiencing mitotic arrest during an acute attempt at regeneration. Less affected hepatocytes appeared vacuolated, and although sometimes randomly distributed, they were more commonly observed in midzonal areas. In contrast, the only histopathological change observed in male phytol-fed mice was multifocal midzonal hepatocyte vacuolation (Fig. 5F). Control-fed male (Fig. 5E) and female (Fig. 5A) mice had no significant lesions. PAS staining of liver sections for glycogen detected no significant histological differences among all groups (not shown).

To define whether phytol feeding altered lipid accumulation in hepatocytes, liver samples were stained with osmium tetroxide and potassium dichromate followed by
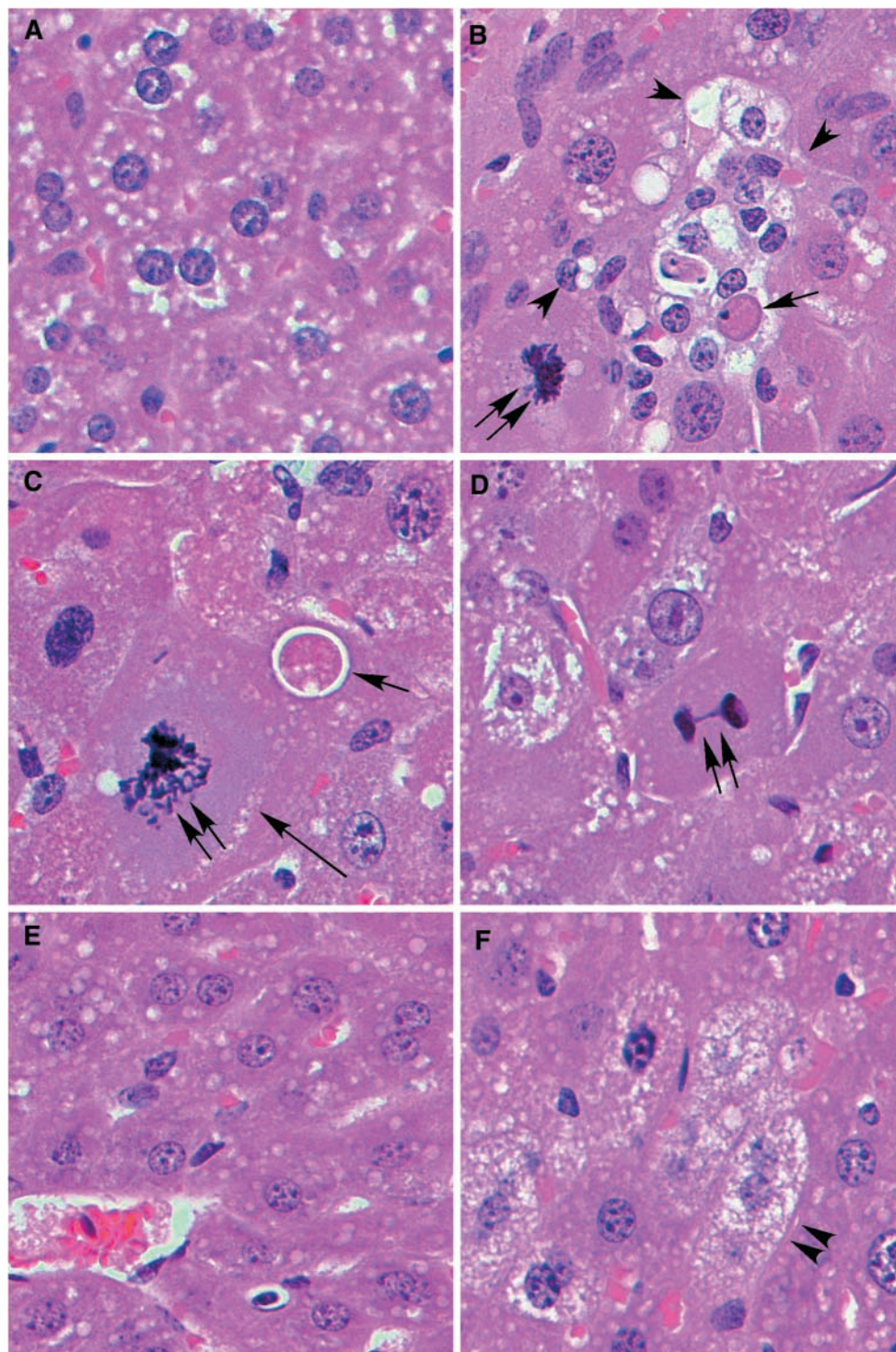
Fig. 5. Liver histopathology. Photomicrographs of representative hematoxylin and eosin-stained sections from control-fed female (A) and male (E) livers show no significant lesions. Liver sections from phytol-fed female mice revealed multifocal microgranulomas (arrowheads in B) with single-cell hepatocyte necrosis or apoptosis (single arrow in B and C), hepatocytomegaly (long arrow in C), and bizarre mitotic figures (two short arrows in B–D). Male phytol-fed mouse livers (F) contained multifocal midzonal hepatocyte vacuolation (double arrowhead) and no other significant lesions. Original magnification, ×400.

examination with TEM, as described in Methods. Two patterns were evident. First, liver hepatocytes of control-fed female mice had more lipid droplets (**Fig. 6A**) than those of control male mice (Fig. 6C). The relative volume density of lipid droplets for control-fed female mice ($16.2 \pm 1.0\%$) was 2.4-fold greater ($P < 0.01$) than that for control-fed males ($6.7 \pm 0.7\%$). Second, liver hepatocytes of control-fed female mice had smaller lipid droplets (Fig.
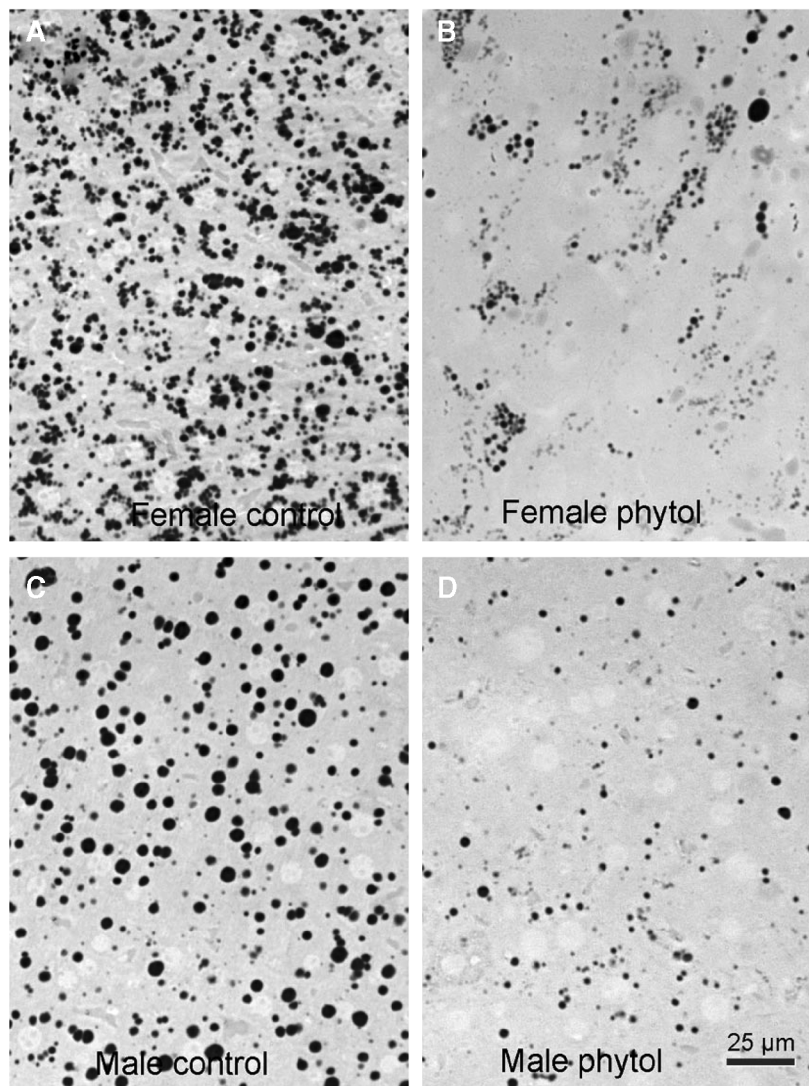
Fig. 6. Quantitative analysis of lipid droplets. Liver sections from female (A and B) and male (C and D) C57BL/6J mice on control (A and C) and phytol (B and D) diets were stained with osmium tetroxide and potassium dichromate to quantitate lipid droplets as described in Methods. Bar = 25 μm.

6A) than those of control male mice (Fig. 6C). The average lipid droplet size for control-fed female mice (11.7 ± 1.4 μm²) was 1.7-fold greater ($P < 0.01$) than that for control-fed males (6.9 ± 0.5 μm²). Third, hepatocytes of phytol-fed females (Fig. 6B) and phytol-fed males (Fig. 6D) both contained fewer lipid droplets than those of the corresponding control-fed mice. The relative volume density of lipid droplets for phytol-fed females (3.7 ± 0.3%) and males (1.4 ± 0.2%) was reduced by 4.4- and 4.8-fold, respectively ($P < 0.01$) compared with that of control-fed females and males. Fourth, hepatocytes of phytol-fed female (Fig. 6B) and phytol-fed male (Fig. 6D) mice both contained smaller lipid droplets than those of the corresponding control-fed mice. The average lipid droplet size for phytol-fed females (5.3 ± 0.6 μm²) and males (3.6 ± 0.2 μm²) was reduced by 2.2- and 1.9-fold, respectively ($P < 0.01$) compared with that for control-fed females and males. These data were consistent with phytol feeding resulting in significantly less neutral lipid in liver hepatocytes.

To define the ultrastructural effects of phytol on hepatocytes, liver samples were stained with DAB for peroxisomes and examined by TEM (**Fig. 7**). Consistent with phytol-induced peroxisomal proliferation of liver enzymes, the size and number of peroxisomes were increased in both males and females on the phytol diet (Figs. 7, 8). A 2.1- and 5.2-fold increase in percentage of total peroxisomes per cell area was observed with the phytol-fed male and female mice, respectively, compared with mice fed the control diet (**Fig. 8A**; $P < 0.05$, n = 5–6). Hepatocytes from females on the phytol diet showed areas of peroxisomal clusters near central veins rather than a random, evenly distributed pattern, as was observed with the phytol-fed male mice (Fig. 8B). Livers from phytol-fed females could not be evaluated near portal veins because of poor staining that was likely attributable to hepatocyte necrosis. Peroxisomes from the female phytol-fed mice appeared more dense and cell membranes were difficult to visualize, most likely indicating hepatocyte degeneration. In summary, liver morphology
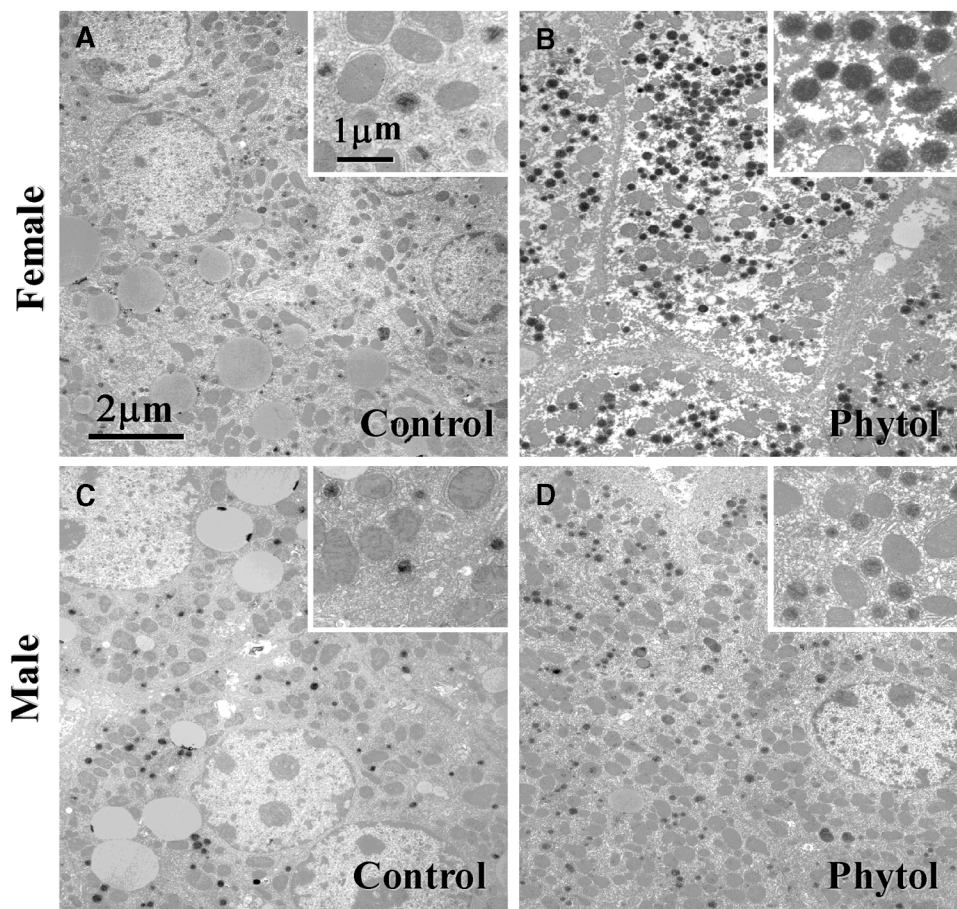
Fig. 7. Transmission electron microscopy. Representative hepatocytes from female (A and B) and male (C and D) C57BL/6J mice on control (A and C) and phytol (B and D) diets were stained with 3,3′-diaminobenzidine to show peroxisomes, which are enlarged in the insets.

was consistent with increased size and numbers of peroxisomes in the phytol-fed animals. Hepatocyte toxicity was apparent only in phytol-fed females, indicating an increased sensitivity to dietary branched-chain fatty acids.

Effect of phytol on the expression of catalase, SCP-2, SCP-x, L-FABP, and FAT/CD36

To further investigate the effect of phytol on peroxisome proliferation, Western blot analysis was performed on liver samples to measure levels of the following peroxisomal proteins: catalase (**Fig. 9A**), SCP-x (Fig. 9D), and SCP-2 (Fig. 9C). Analysis of multiple Western blots showed that levels of catalase were increased by 2.0- and 2.1-fold in phytol-fed males and females, respectively, compared with control-fed males and females (Fig. 9H), consistent with the results presented in Histopathology (Figs. 7, 8). Expression of SCP-2 was increased by 1.8-fold in both male and female phytol-fed mice (Fig. 9G). SCP-x levels increased by up to 4.4- and 1.5-fold in phytol-fed females and males, respectively (Fig. 9G). Although basal levels of SCP-x were almost 6-fold lower in females versus males on the control diet, phytol feeding increased the level of SCP-x in female mice, but still by 20% less than that of control-fed males and 180% less than that of phytol-fed males.

Because plasma membrane FAT/CD36 and cytosolic L-FABP are known to be involved in the uptake and intracellular transport of fatty acids, the effect of phytol diets on levels of these proteins was determined. Phytol feeding increased liver levels of L-FABP by up to 1.9-fold in both males and females (Fig. 9B, G). In contrast, levels of FAT/CD36 were increased by 2.2-fold in males only, with no change observed in females (Fig. 9E, H).

Because the nuclear regulatory protein PPARα (Fig. 9F) is activated by phytanic acid and fibrates to increase the transcription of catalase, L-FABP, FAT/CD36, and peroxisomal oxidative enzymes [reviewed in ref. (43)], Western blotting was performed to determine if phytol-induced proliferation of peroxisomes affected PPARα expression level. Phytol diets decreased the level of PPARα in the livers of females by 3.3-fold, whereas no change was observed in males (Fig. 9H).

In summary, phytol diets increased the levels of catalase, SCP-2, and SCP-x, consistent with peroxisomal proliferation in liver. In addition, phytol diets also induced the expression of two other transport proteins, L-FABP and FAT/CD36 (males only). These data were consistent with phytol acting through its metabolite (phytanic acid) to interact with PPARα and activate the transcription of PPARα-
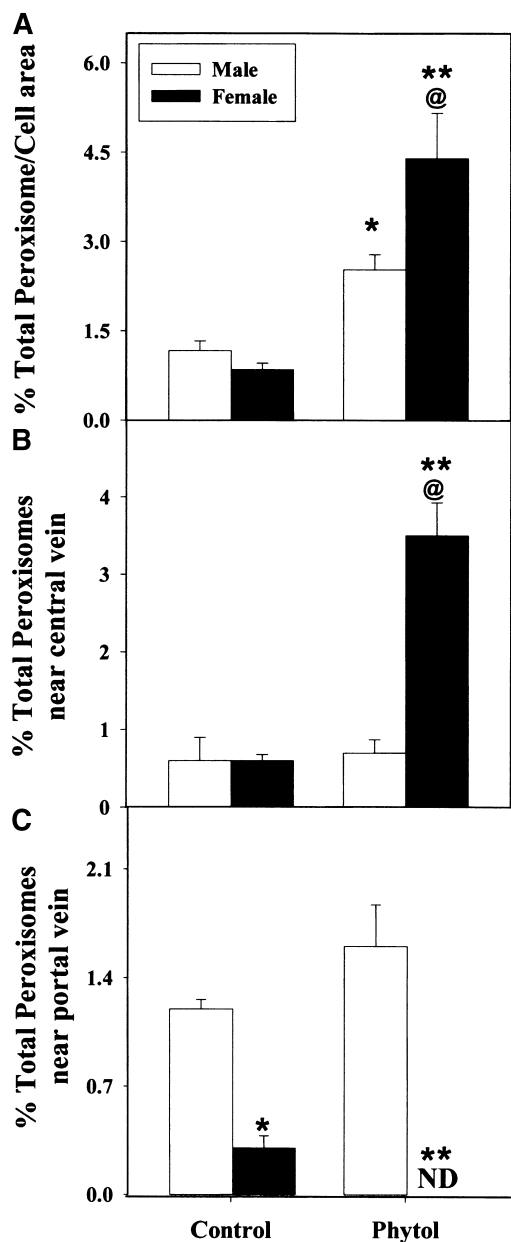
A

B

C

Fig. 8. Quantitation of peroxisomes in liver. The percentage total peroxisomes per cell area (A), percentage total peroxisomes near the central vein (B), and percentage total peroxisomes near the portal vein (C) were calculated using morphometric analysis as described in Methods. Values represent means ± SEM. * $P < 0.05$ (n = 5–6) compared with males on the control diet. ** $P < 0.05$ (n = 5–6) compared with males on the phytol diet. @ $P < 0.05$ (n = 5–6) compared with females on the control diet. ND, not detected.

regulated genes (44, 45). These increases were evident in both males and females, even though phytol-fed females exhibited significantly reduced levels of PPARα and no change of FAT/CD36.

Effect of phytol on liver lipids

To determine any changes in liver lipid compositions among groups, lipids were extracted and analyzed as de-

scribed in Methods. Although liver unesterified fatty acid levels did not differ between control-fed females and males (data not shown), total esterified lipids (e.g., triglycerides, phospholipids, cholesteryl esters) were 2-fold higher in livers of females than males (**Table 1**). The higher total esterified lipid of the female mice was not attributable to altered phospholipid content, consistent with the fact that control females and males did not differ in the quantity of membranous structures such as peroxisomes (Fig. 7A vs. 7C). Total neutral lipids were 3- to 4-fold higher in livers of control females versus males, consistent with TEM observations (Fig. 6A vs. 6C). The higher total neutral lipid level in the female livers was primarily attributable to 2.3- and 3.5-fold higher levels of cholesteryl esters and triacylglycerides. Thus, the higher amount of neutral lipids in female livers on the control diet was distributed throughout the liver hepatocytes, apparently in the form of lipid droplets (Fig. 6A).

Phytol feeding reduced the level of unesterified fatty acids in liver of females compared with males (21.0 ± 0.9 vs. 39.2 ± 4.1 nmole/mg protein; $P < 0.01$, n = 5–6). This finding may account for the reduced levels of PPARα in livers of phytol-fed females (Fig. 9H). Phytol feeding did not alter total lipid levels in livers of male mice (Table 1), but resolution into individual esterified lipid classes revealed subtle differences. Liver total phospholipid levels were 1.7-fold increased in phytol-fed males compared with control males, consistent with increased proliferation of membranous structures (e.g., peroxisomes; Fig. 8A). In contrast, total neutral lipid was 3.2-fold decreased in livers of phytol-fed versus control-fed females (Table 1). The lower total neutral lipid level was primarily associated with triacylglyceride, which was decreased by 54% in phytol-fed females. Although cholesteryl ester levels in mice were severalfold lower than those of triacylglycerides, phytol feeding oppositely affected cholesteryl ester levels in livers of females (i.e., 1.5-fold increased cholesteryl ester). Livers of control-fed males and females did not significantly differ in cholesterol content. Although phytol feeding did not significantly alter liver cholesterol in males, phytol-fed females had 1.5-fold ($P < 0.04$, n = 5–6) higher cholesterol. However, the ratio of cholesterol to phospholipid did not differ between male and female livers from either control-fed or phytol-fed animals.

In summary, regardless of diet, livers from female mice contained more total lipid, especially neutral lipids (both cholesteryl ester and triacylglyceride) than those of males. Although phytol feeding did not alter liver total lipid levels in either females or males, individual lipid classes revealed significant differences. Phytol-fed females and males exhibited increased levels of total phospholipid, whereas neutral lipids were decreased compared with controls. Further resolution of individual neutral lipid classes detected a sexual dimorphic response to phytol diets. Although phytol feeding significantly decreased the triacylglycerol levels in livers of both males and females, liver cholesteryl ester levels were increased in female but not male mice. Taken together, these data confirmed the morphometric analysis of what was indicated grossly and mi-
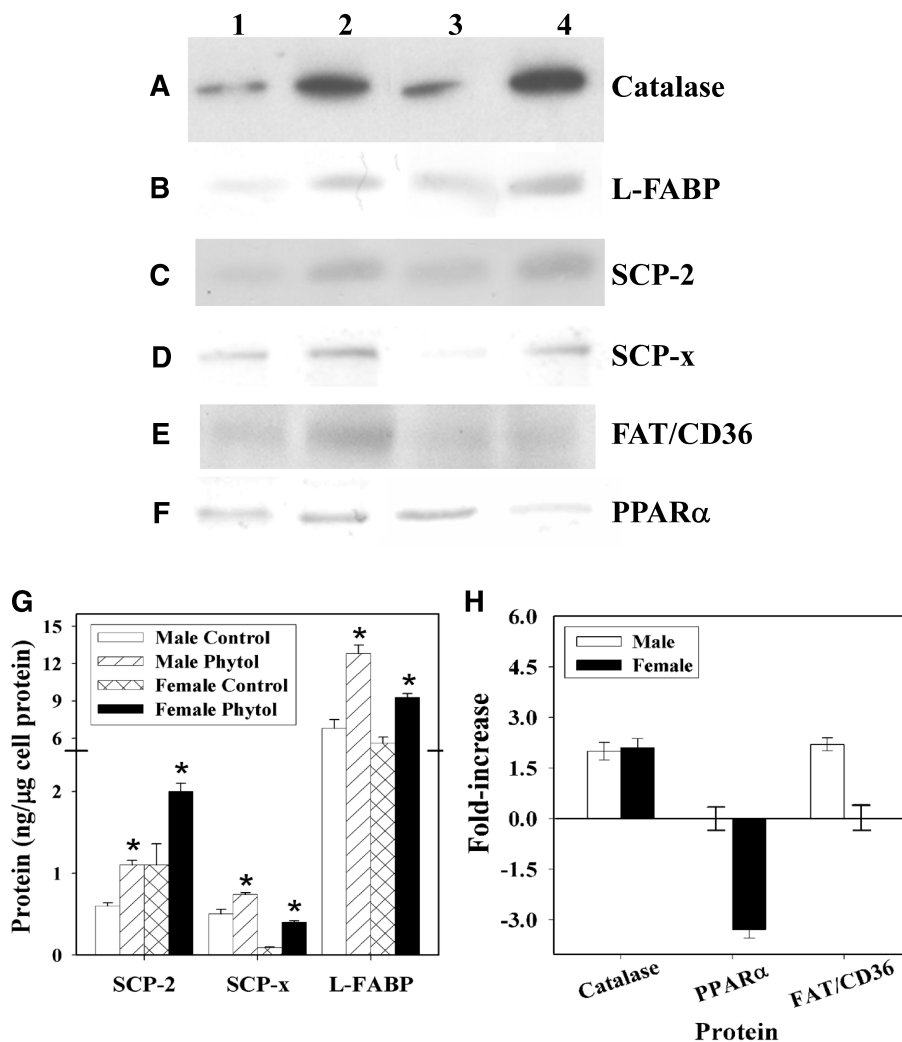
Fig. 9. Liver protein quantitation. Levels of catalase (A), liver fatty acid binding protein (L-FABP; B), sterol carrier protein-2 (SCP-2; C), SCP-x (D), fatty acid translocase (FAT)/CD36 (E), and peroxisome proliferator-activated receptor α (PPARα; F) were determined by Western blot analysis in male (lanes 1 and 2) and female (lanes 3 and 4) mice fed control (lanes 1 and 3) and phytol (lanes 2 and 4) diets as described in Methods. Quantitation (G) and fold increase (H) in hepatic protein levels of SCP-2, SCP-x, L-FABP, catalase, PPARα, and FAT/CD36 were also determined. Values represent means ± SEM. * $P < 0.05$ (n = 5–6) compared with males on the control diet.

croscopically (i.e., that the amount of neutral lipid droplets was greatly reduced in the phytol-fed mice, especially females).

Effect of phytol on serum lipids

To determine if the higher total neutral lipids (both cholesteryl ester and triacylglycerol) in control females correlated with lower serum neutral lipid levels, serum was analyzed as described in Methods. Although serum unesterified fatty acid levels did not significantly differ between males (21.3 ± 3.4 nmol/mg protein) and females (19.7 ± 2.3 nmol/mg protein), serum total lipid was 30% lower ($P < 0.05$, n = 5–6) in females, primarily by 40, 27, and 63% lower levels of phospholipid, triacylglyceride, and cholesterol, respectively (Table 1; $P < 0.05$, n = 5–6).

Because phytol stimulated more peroxisome proliferation in livers of females, serum lipids were measured in

phytol-fed mice. Phytol feeding decreased the serum level of unesterified fatty acids by 2-fold in both males (11.0 ± 1.7 nmol/mg protein vs. 21.3 ± 3.4 nmol/mg protein; $P < 0.05$) and females (9.9 ± 2.2 nmol/mg protein vs. 19.7 ± 2.3 nmol/mg protein, $P < 0.05$). Phytol-fed female mice exhibited decreased serum total lipid, total neutral lipid, cholesteryl ester, and triacylglyceride levels, but not cholesterol, compared with control-fed females (Table 1). In contrast, phytol-fed males had decreased levels of serum triacylglyceride; in addition, total lipid, phospholipid, and cholesterol tended to decrease. In contrast, phytol-fed males had unaltered serum levels of total neutral lipid and cholesteryl ester (Table 1). Thus, serum total lipid was lower in females and preferentially decreased in phytol-fed females. This finding was consistent with the greater liver peroxisome proliferative effect of phytol in females.

TABLE 1. Esterified lipids in liver and serum in mice fed a defined diet with or without 0.5% phytol

Lipids	Male		Female	
	Control	Phytol	Control	Phytol
	nmol/mg protein			
Liver				
Cholesteryl ester	74.11 ± 8.0	58.9 ± 5.7	167.6 ± 19.2[a]	261.2 ± 49[b,c]
Triglyceride	396.9 ± 45.3	89.8 ± 14.6[a]	1,340 ± 103[a]	643.1 ± 58.2[b,c]
Cholesterol	41.85 ± 3.4	36.5 ± 2.0	46.7 ± 8.2	70.2 ± 6.3[b,c]
Phospholipid	487.26 ± 29.3	858.7 ± 130[a]	549.9 ± 58.8	862.2 ± 3.9[c]
Neutral lipids	471.0 ± 46	148.7 ± 15.7[a]	1507 ± 104[a]	904.3 ± 76[b,c]
Total lipids	1,026 ± 55.4	1,083 ± 132	2,131 ± 121[a]	1,857.7 ± 80[b]
Serum				
Cholesteryl ester	90.9 ± 7.8	111.7 ± 9.2	82.8 ± 5.6	48.9 ± 4.0[b,c]
Triglyceride	8.2 ± 0.75	2.8 ± 0.09[a]	6.0 ± 0.74	3.1 ± 0.40[c]
Cholesterol	19.3 ± 3.1	14.0 ± 1.2	7.2 ± 1.3[a]	9.0 ± 0.62[b]
Phospholipid	146.3 ± 17.4	96.47 ± 6.7[a]	88.4 ± 8.2[a]	72.5 ± 3.2[b,c]
Neutral lipids	99.2 ± 7.8	114.4 ± 9.22	88.8 ± 5.7	52.0 ± 4.0[b,c]
Total lipids	286.0 ± 19.6	235.9 ± 11.6	204.0 ± 10.3[a]	143.4 ± 5.9[b,c]

Values represent means ± SEM.
[a] $P < 0.05$ (n = 5–6) compared with males on the control diet.
[b] $P < 0.05$ (n = 5–6) compared with males on the phytol diet.
[c] $P < 0.05$ (n = 5–6) compared with females on the control diet.

Differential metabolism of branched-chain fatty acids

To determine if female mice metabolized phytol differently than males, liver lipids were extracted, esterified lipids were transesterified to form FAMEs, and FAMEs were analyzed by gas-liquid chromatography to determine the relative levels of the respective metabolites described above.

In livers of both female and male mice on control diets, phytanic acid was detected at similar low levels (0.1% of esterified lipid; **Fig. 10A**). In contrast, phytanic acid con-
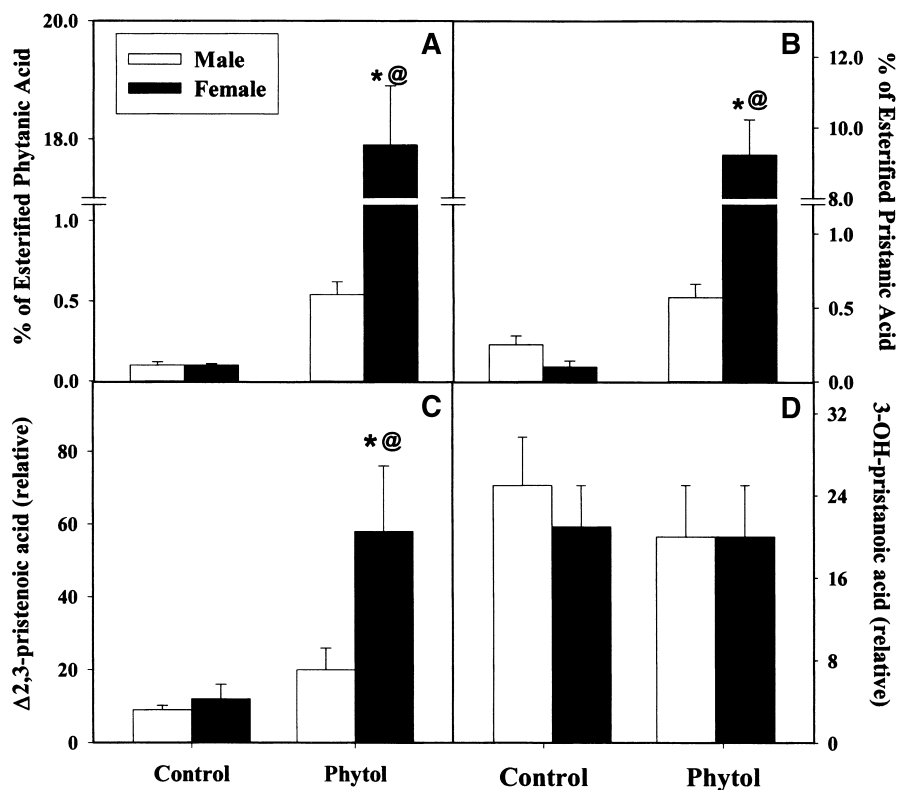
Fig. 10. Phytanic acid, pristanic acid, Δ-2,3-pristenoic acid, and 3-OH-pristanoic acid levels in liver. Hepatic levels of phytanic acid (A), pristanic acid (B), Δ-2,3-pristenoic acid (C), and 3-OH-pristanoic acid (D) were determined in male and female mice on control and phytol diets as described in Methods. Values represent means ± SEM. * $P < 0.01$ (n = 5–6) compared with females on the control diet. @ $P < 0.01$ (n = 5–6) compared with males on the phytol diet.

stituted 0.5% and 18% of esterified lipids in phytol-fed males and females, respectively (Fig. 10A). Compared with controls, phytol-fed males and females had 5- and 180-fold higher phytanic acid levels in esterified lipids. Thus, phytol-fed females accumulated 30-fold more phytanic acid in esterified form than did phytol-fed males. A similar pattern of phytanic acid accumulation was observed in serum of phytol-fed females versus males (data not shown). Because phytol-fed females accumulated much higher levels of the first (i.e., extraperoxisomal) metabolite of phytol (phytanic acid) than did males, extraperoxisomal formation of phytanic acid was not defective in females compared with males. Instead, the data suggested a downstream block in peroxisomal α- or β-oxidation or in thiolytic cleavage of the branched-chain 3-keto-pristanoyl-CoA, a step catalyzed specifically by SCP-x.

To examine whether females also accumulated peroxisomal phytanic acid metabolites, the level of pristanic acid (the product of peroxisomal α-oxidation of phytanoyl-CoA) was examined. Liver levels of esterified pristanic acid in control-fed males and females were near 0.2–0.3% of total esterified fatty acids (Fig. 10B), essentially the same as or only slightly higher than the levels of phytanic acid (Fig. 10A). In contrast, in phytol-fed males and females, pristanic acid constituted 0.5% and 9% of total esterified fatty acids, 5- and 92-fold higher than the levels in control-fed males and females, respectively (Fig. 10B). A similar trend of pristanic acid accumulation was also observed in serum lipids (data not shown). Because livers of phytol-fed female mice accumulated 18-fold more pristanic acid (the first peroxisomal metabolite of phytanic acid) than did livers of phytol-fed males (Fig. 10B), peroxisomal α-oxidation to form pristanic acid was not defective in females compared with males. Instead, the data suggested a downstream block in peroxisomal β-oxidation or in thiolytic cleavage of the branched-chain 3-keto-pristanoyl-CoA, a step catalyzed specifically by SCP-x.

With regard to the peroxisomal β-oxidation products of pristanic acid, analysis by mass spectrometry showed that the levels of Δ-2,3-pristenoic acid (Fig. 10C) and 3-OH-pristanoic acid (Fig. 10D) in liver lipids did not differ between control-fed males and females. In contrast, liver lipids of male and female phytol-fed mice had 1.7- and 5-fold higher levels of Δ-2,3-pristenoic acid, respectively, compared with control-fed male and female mice (Fig. 10C). Again, female phytol-fed mice accumulated 2.9-fold more metabolite (i.e., Δ-2,3-pristenoic acid) than did phytol-fed males (Fig. 10C). In contrast, levels of 3-OH-pristanoic acid in liver lipids of phytol-fed males and females did not differ from those of control-fed mice or between male and female mice (Fig. 10D). Because of their instability, the last intermediate (i.e., 3-ketopristanoyl-CoA) before thiolytic cleavage by SCP-x was not detectable by mass spectrometry, an observation consistent with the findings of others (12).

In summary, female mice on control diets and even more markedly on phytol diets accumulated significantly higher levels of almost all detectable phytol metabolites before thiolytic cleavage of 3-ketopristanoyl-CoA medi-

ated specifically by SCP-x. This was consistent with the substantially lower levels of SCP-x in livers of females than males, whether control-fed or phytol-fed. Thus, the females' highly increased accumulation of phytol metabolites before the thiolytic cleavage step mediated by SCP-x may be attributable, at least in part, to their reduced levels of SCP-x compared with that in males.

Effect of phytol on the levels of other liver esterified fatty acids

The content of phytol metabolites in livers of male and female control-fed mice did not differ, but the mass content of other fatty acids in liver was significantly different between control males and females (**Table 2**). Mass levels of almost all fatty acids were higher in liver lipids of control females compared with control males. This finding was consistent with the higher content of esterified lipids (especially triacylglycerides and cholesteryl esters) noted in control-fed females (Table 1). Phytol feeding decreased the mass of nearly all liver fatty acids, especially those of females (Table 2). These data were consistent with the lower content of esterified lipids in livers of phytol-fed female versus male mice noted previously (Table 1). When these data were expressed as total mass of different classes of fatty acids (e.g., PUFAs, MUFAs, PUFA/MUFA ratio, unsaturated, saturated, saturated-unsaturated ratio), several significant differences were observed. Phytol feeding significantly decreased the mass content of PUFAs, MUFAs, and saturated and unsaturated fatty acids in liver lipids of male mice by severalfold (Table 2). Differences in fatty acid mass were even more pronounced in liver lipids of female phytol-fed mice compared with control-fed mice, in which 2.0-, 4.3-, and 2.9-fold decreases in mass of liver PUFAs, MUFAs, and unsaturated fatty acids, respectively, were observed. In addition, phytol feeding increased the saturated-unsaturated and PUFA/MUFA ratios by 2.7- and 2.1-fold, respectively, in the female mice (Table 2). A high proportion of saturated fatty acids in esterified lipids is known to be associated with liver morphometric alterations indicative of toxicity (46), changes potentiated by peroxisome proliferators (47).

Effect of phytol on the levels of serum esterified fatty acids

To determine if phytol-induced alterations in liver fatty acid mass and composition were also reflected in serum lipids, the mass of fatty acids was examined. The serum mass of almost all esterified fatty acids, other than phytol metabolites, was the same or slightly lower in control-fed females versus males (**Table 3**). These findings were consistent with the lower content of total esterified lipids (primarily phospholipids and triacylglycerides) in serum of control-fed female mice (Table 1). When these data were expressed as total mass of different classes of fatty acids (e.g., PUFAs, MUFAs, PUFA/MUFA ratio, unsaturated, saturated, saturated-unsaturated ratio), however, no significant differences were observed in serum esterified fatty acids of male and female mice on control diets.

TABLE 2. Liver esterified fatty acid mass in mice fed a defined diet with or without 0.5% phytol

Fatty Acid	Male		Female	
	Control	Phytol	Control	Phytol
	nmol/mg protein			
14:0	5.6 ± 0.9	2.07 ± 0.3	19.1 ± 3.9	8.24 ± 4.7
14:1 n-5	0.6 ± 0.2	0.2 ± 0.04	1.4 ± 0.27	0.5 ± 0.1
16:0	208.7 ± 24.7	124.3 ± 12.2	619.5 ± 73.6	246.6 ± 17.6
16:1 n-7	36.1 ± 3.3	12.3 ± 2.1	111.6 ± 20.8	32.4 ± 3.9
18:0	59.7 ± 4.8	52.9 ± 4.8	125.7 ± 13.71	111.8 ± 9.7
18:1 n-9	235.6 ± 26.07	78.5 ± 10.9	796.9 ± 108	151.1 ± 12.7
18:2 n-9,12	194.4 ± 33.1	84.02 ± 10.4	553.52 ± 59.1	228.7 ± 20.1
18:3 α-n-6,9,12	3.7 ± 0.98	1.12 ± 0.62	ND	1.58 ± 0.18
18:3 γ-n-6,9,12	8.6 ± 1.3	2.1 ± 0.35	24.1 ± 2.4	7.25 ± 0.74
20:0	2.0 ± 0.41	0.75 ± 0.13	0.9 ± 0.20	4.5 ± 0.33
20:1 n-11	9.47 ± 1.9	2.63 ± 0.44	7.6 ± 0.9	10.5 ± 0.98
20:2 n-11,14	1.44 ± 0.24	0.36 ± 0.07	3.2 ± 0.5	3.9 ± 1.2
20:4	80.9 ± 6.3	71.1 ± 6.8	123.0 ± 11.2	77.4 ± 10.9
22:0	1.6 ± 0.25	0.88 ± 0.13	0.9 ± 0.11	2.4 ± 0.48
22:1 n-13	2.6 ± 1.0	1.0 ± 0.34	2.06 ± 0.59	3.46 ± 0.23
24:0	1.6 ± 0.41	0.73 ± 0.10	1.48 ± 0.15	5.5 ± 0.35
22:4	3.5 ± 0.42	1.6 ± 0.17	5.35 ± 1.15	8.6 ± 0.82
24:1 n-9	4.5 ± 2.3	3.2 ± 1.8	2.21 ± 0.34	6.3 ± 0.65
22:6	27.7 ± 3.2	21.5 ± 2.4	54.7 ± 5.12	46.9 ± 3.88
Phytanic acid	0.94 ± 0.16	2.6 ± 0.36	2.8 ± 0.3	244.4 ± 13.1
Pristanic acid	2.2 ± 0.59	2.8 ± 0.4	2.4 ± 0.9	125.8 ± 13.8
Sat/protein	285.7 ± 25.2	189.8 ± 13.16[a]	784.67 ± 75[a]	751.4 ± 28[b]
Unsat/protein	646.2 ± 43.1	297.3 ± 17.0[a]	1758.2 ± 126[a]	611.7 ± 26.9[a,b]
MUFA/protein	314.6 ± 26.6	107.3 ± 11.3[a]	970.6 ± 110[a]	223.1 ± 13.9[a]
PUFA/protein	331.6 ± 33.9	189.9 ± 12.7[a]	787.6 ± 61.8[a]	388.6 ± 23.3[b]
Ratios	*nmol/nmol*			
Sat/Unsat	0.44 ± .05	0.64 ± .06	0.45 ± 0.05	1.23 ± 0.07[b]
PUFA/MUFA	1.0 ± .14	1.8 ± 0.22[a]	0.81 ± 0.11	1.74 ± 0.15[a]

ND, not detected; Sat, saturated fatty acid; Unsat, unsaturated fatty acid. Values represent means ± SEM.
[a] $P < 0.05$ (n = 3–6) compared with mice fed a control food.
[b] $P < 0.05$ (n = 3–6) compared with male mice fed a phytol diet.

Phytol feeding decreased the mass of nearly all serum esterified fatty acids in female, but not male, mice (Table 3). These results were consistent with the lower content of esterified lipids in serum of phytol-fed female versus male mice noted above (Table 1). When expressed as total mass of different classes of fatty acids (e.g., PUFAs, MUFAs, PUFA/MUFA ratio, unsaturated, saturated, saturated-unsaturated ratio), several additional significant differences were observed. Phytol feeding significantly decreased the mass content of PUFAs, MUFAs, and unsaturated fatty acids in serum lipids of females by 54, 66, and 59%, respectively, but not in males (Table 3). Even when expressed as percentage composition, phytol feeding significantly altered the percentage of these classes of esterified fatty acids in serum of females but not males, such that the levels of MUFAs and unsaturated fatty acids were decreased by 40% and 29%, respectively, whereas the percentage proportion of saturated esterified fatty acids and the saturated-unsaturated ratio were increased by 1.5- and 2.2-fold, respectively (data not shown). Thus, although serum esterified fatty acids were not significantly different between control males and females, the phytol diet significantly decreased these levels in females. This result was reflected in the decreased PUFAs and MUFAs in female phytol-fed mice (Table 3). Despite the decreased values of 16:0 and 18:0, overall saturated levels were not decreased, attributable to the large concomitant increases in the levels of phytanic acid and pristanic acid in the females fed phytol (Table 3).

Effect of clofibric acid on liver weight, triglyceride levels, and protein expression

It has not been established whether the effects of phytol were similar to those of other peroxisomal proliferators (i.e., clofibrates) acting through the nuclear hormone receptor PPARα. Clofibrate is known to stimulate PPARα and thereby enhance the expression of enzymes associated with peroxisomal fatty acid oxidation (43). The effects of a 0.2% clofibric acid (the metabolically active form of clofibrate) diet on liver weights, triglyceride levels, and the ability to stimulate the expression of several proteins associated with fatty acid oxidation (L-FABP, SCP-2, and SCP-x) were determined (**Fig. 11**). Similar to results from mice fed the 0.5% phytol diet, liver weights increased significantly in the clofibric acid-fed male and female mice attributable to the proliferative effects of the fibrates (Fig. 11A). A hypotriglyceridemic effect was also observed, in which liver levels of triglycerides decreased by 58% and 71%, respectively, in male and female mice fed clofibric acid (Fig. 11B; $P < 0.02$, n = 5–6). A similar hypotrigliceridemic pattern in response to clofibrate was also observed in serum of both male and female mice (not shown). In addition, levels of cytosolic L-FABP, along with SCP-2, increased, suggesting that upregulation was mediated by clofibric acid in

TABLE 3. Serum esterified fatty acid mass in mice fed a defined diet with or without 0.5% phytol

Fatty Acid	Male		Female	
	Control	Phytol	Control	Phytol
	nmol/mg protein			
14:0	0.78 ± 0.17	0.35 ± 0.13	1.0 ± 0.4	0.53 ± 0.3
14:1 n-5	0.14 ± 0.02	1.76 ± 0.55	0.62 ± 0.15	0.52 ± 0.21
16:0	36.6 ± 5.0	31.6 ± 2.0	27.8 ± 5.2	14.4 ± 1.4
16:1 n-7	3.47 ± 1.0	1.96 ± 0.49	1.55 ± 0.21	0.94 ± 0.15
18:0	13.78 ± 1.96	14.63 ± 0.76	14.74 ± 2.74	5.6 ± 1.6
18:1 n-9	14.1 ± 3.5	12.8 ± 1.4	12.3 ± 1.6	6.47 ± 1.4
18:2 n-9,12	23.5 ± 6.5	24.5 ± 2.6	18.1 ± 2.8	10.8 ± 1.7
18:3 α-n-6,9,12	0.76 ± 0.28	0.48 ± 0.11	ND	0.62 ± 0.29
18:3 γ-n-6,9,12	1.13 ± 0.28	0.81 ± 0.10	0.95 ± 0.11	0.23 ± 0.02
20:0	0.24 ± 0.10	0.20 ± 0.05	0.42 ± 0.13	0.20 ± 0.12
20:1 n-11	0.37 ± .10	0.27 ± 0.04	0.67 ± 0.37	0.18 ± 0.03
20:2 n-11,14	0.69 ± 0.22	0.21 ± 0.07	1.11 ± 0.81	0.36 ± 0.17
20:4	24.8 ± 6.2	29.4 ± 2.6	18.8 ± 2.9	5.8 ± 1.23
22:0	0.33 ± 0.12	ND	0.51 ± 0.40	ND
22:1 n-13	ND	0.31 ± 0.07	0.24 ± 0.10	ND
24:0	ND	ND	ND	ND
22:4	0.34 ± 0.11	0.64 ± 0.20	0.62 ± 0.20	0.33 ± 0.20
24:1 n-9	1.10 ± 0.60	1.44 ± 0.40	1.22 ± 0.55	2.4 ± 1.22
22:6	3.84 ± 1.2	4.21 ± 0.74	5.73 ± 1.71	2.32 ± 0.98
Phytanic acid	0.36 ± 0.10	0.81 ± 0.08	0.91 ± 0.39	16.78 ± 3.36
Pristanic acid	ND	0.79 ± 0.30	ND	2.48 ± 0.44
Sat/protein	53.55 ± 5.41	49.55 ± 2.18	48.85 ± 6.02	40.56 ± 4.02
Unsat/protein	77.83 ± 9.87	82.96 ± 4.10	76.10 ± 6.46	31.0 ± 2.9[a,b]
MUFA/protein	21.26 ± 3.72	20.85 ± 1.76	29.59 ± 4.65	10.18 ± 1.77[a]
PUFA/protein	56.07 ± 9.14	62.1 ± 3.7	46.5 ± 4.49	20.81 ± 2.4[a,b]
Ratios		*nmol/nmol*		
Sat/Unsat	0.69 ± 0.11	0.60 ± 0.04	0.64 ± 0.10	1.31 ± 0.18[a,b]
PUFA/MUFA	2.64 ± 0.63	2.98 ± 0.31	1.57 ± 0.29	2.04 ± 0.42

Values represent means ± SEM.
[a] $P < 0.05$ (n = 3–6) compared with mice fed a control food.
[b] $P < 0.05$ (n = 3–6) compared with male mice fed a phytol diet.

response to the activation of PPARα. These results were consistent with those observed with mice fed a phytol diet, indicating that similar mechanisms are involved.

DISCUSSION

Although a variety of correlative studies, as well as experiments performed in vitro and with transfected cells, indicate that SCP-x and SCP-2 may be involved in the metabolism of fatty acids (48), their full significance has not been demonstrated. In particular, the physiological relevance of SCP-x in branched-chain fatty acid metabolism has yet to be resolved. To begin to address this issue, it was important to use a physiological system in which SCP-x levels were low or absent, as observed with the results presented here with female C57BL/6J mice, in which liver levels of SCP-x were 5-fold lower than those of their male counterparts. Furthermore, lower liver SCP-x levels in females were not strain or species specific, having been observed in C57BL/6J mice (present work), FVB mice (not shown), BALB/c mice (30), and rats (49, 50). These findings suggest that female mice could serve as a natural in vivo model system for SCP-x deficiency/reduction. The intrinsically lower liver SCP-x levels of female versus male mice suggested that female mice might be much less able to metabolize branched-chain fatty acids and might also be more sensitive to the subsequent adverse effects of fatty acid buildup. The present work, using C57BL/6J male and female mice, provided several new insights regarding the role of SCP-x in branched-chain fatty acid metabolism.

The gross phenotype of female mice was altered much more in response to dietary phytol than that of male mice. Phytol-fed females lost, rather than gained, body weight, exhibited decreased body fat tissue mass, and had gross and histological lesions of hepatotoxicity. The latter was especially evident in the livers of phytol-fed females, which had gross swelling with paleness and mottling, suggestive of necrosis (cell death and edema) and/or steatosis (fatty change with increased lipids). Because the protein-liver weight ratio remained relatively constant compared with that in controls, liver enlargement exclusively attributable to peroxisomal proliferation was ruled out when weight was adjusted for protein content. This result, combined with the fact that the levels of total neutral lipids and lipid droplets both decreased, was consistent with necrosis rather than steatosis, a finding confirmed by histopathological examination. TEM morphometric histological and lipid analyses confirmed peroxisomal proliferation concomitant with liver necrosis in the phytol-fed female mice and peroxisomal proliferation without necrosis in the phytol-fed males. These findings represent the first demonstration of sexual dimorphism in response to dietary branched-chain phytol, a precursor of phytanic acid.
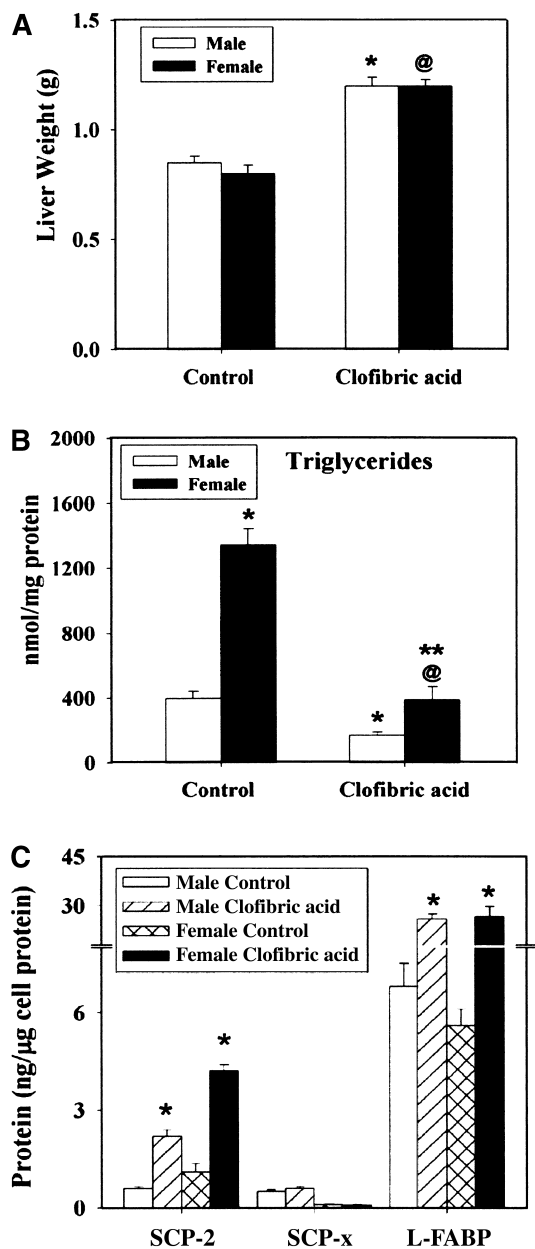
Fig. 11. Effect of clofibrates on C57BL/6J male and female mice. Liver weight (A), triglyceride levels (B), and expression of SCP-2, SCP-x, and L-FABP (C) were determined in male and female mice on control and clofibric acid diets as described in Methods. Values represent means ± SEM. * $P < 0.01$ (n = 5–6) compared with females on the control diet. ** $P < 0.05$ (n = 5–6) compared to males on the clofibric acid diet. @ $P < 0.01$ (n = 5–6) compared with males on the phytol diet.

Phytol feeding induced peroxisome proliferation in both male and female mice, consistent with the accumulation of phytanic acid and its metabolites. Levels of peroxisomal proteins (i.e., catalase, SCP-x, SCP-2) and extraperoxisomal proteins (i.e., L-FABP, SCP-2, FAT/CD36) were increased. Phytanic acid is a known ligand of PPARα (44), which in turn induces the expression not only of the peroxisomal protein catalase but also of many other proteins involved in peroxisomal fatty acid oxidation, including L-FABP. The work presented here showed for the first time

that SCP-x and SCP-2 were also induced by phytanic acid. Because both promoters in the SCP-2 gene contain an imperfect DR-1 element (51), a potential binding region for PPARα, these results suggest potential gene regulation by PPARα. In addition, because SCP-x, SCP-2, and L-FABP have high affinity for phytanic acid (44, 52), these results are consistent with these proteins being regulated by their fatty acid substrates in a manner similar to many enzymes involved in peroxisomal fatty acid oxidation (52). Moreover, because SCP-x, SCP-2, L-FABP, and FAT/CD36 enhance fatty acid uptake (28, 53–55) and SCP-x, SCP-2, and L-FABP enhance intracellular transport (26, 56) and peroxisomal fatty acid oxidation (28, 57), increased expression may reduce the toxic threshold of phytol by relieving the fatty acid load in the cell. However, the decreased liver SCP-x level of female versus male mice was shown to result in reduced capacity to handle high doses of phytanic acid despite the upregulation of SCP-2 and L-FABP. Consistent with these results, when SCP-x is absent, as with the SCP-x/SCP-2 knockout mouse, enhanced phytol toxicity was observed despite the upregulation of the L-FABP gene product (12). The greater response of female versus male mice to a phytol diet was consistent with the accumulation of high levels of phytanic acid and its metabolites in females. The intrinsically lower level of SCP-x in female mice most likely led to the higher accumulation of phytanic acid and pristanic acid in phytol-fed females versus males. Although phytol feeding increased the level of SCP-x in male and female mice, the levels of SCP-x in phytol-fed females was still significantly lower than that in phytol-fed males. These levels were insufficient to adequately metabolize phytol and most likely contributed to the greater accumulation of phytanic acid and phytanic acid metabolites in phytol-fed female versus male mice. These data were consistent with the PPARα ligand phytanic acid acting as a transactivator of SCP-x, despite the fact that levels of PPARα itself were not increased; instead, they were decreased by 2-fold in the phytol-fed female mice. PPARα null mice showed opposite liver abnormalities: fatty liver on either fasting or high-fat diets (58, 59). Therefore, it is unlikely that the reduction in PPARα observed in phytol-fed females was responsible for the decreased liver lipid accumulation (i.e., fewer lipid droplets, less neutral lipid) in phytol-fed females and males. Taken together, these data suggested that the greater susceptibility of females to phytol was consistent with the fact that phytanic acid, the first metabolite of phytol, accumulated to much higher levels in female than male mice.

Phytanic acid, as ligand to PPARα, induced the expression not only of peroxisomal proteins (catalase) and fatty acid transport proteins (L-FABP, FAT/CD36) but also of SCP-2 and SCP-x. Although these effects resulted in the overall induction of peroxisomal fatty acid oxidation, the level of SCP-x in phytol-fed females was still significantly lower than that of males. Thus, the lower intrinsic level of SCP-x, as well as the lower phytol-induced level of SCP-x in females, likely contributed to the greater liver injury observed in livers of phytol-fed female livers. However, given the complexity of working with animal models, it is not

possible to directly assign cause and effect without considering other compensatory mechanisms. In particular, different groups of transport proteins, including those involved in plasma membrane (FAT/CD36) and cytosolic (L-FABP and SCP-2) fatty acid transport, were examined in phytol-fed male versus female mice to determine whether factors other than the intrinsically lower liver SCP-x levels of female mice could account for the results observed. None of these proteins showed changes that could accommodate the observed decreased ability of female mice to oxidize phytanic acid. This was particularly relevant given the observation that female mice (with 5-fold lower SCP-x levels) and SCP-x/SCP-2 gene-ablated mice (null in SCP-x and SCP-2) exhibited several similar phenotypes, including impaired body weight control and an impaired ability to catabolize methyl-branched fatty acids when phytol was supplemented to the diet (12). In addition, SCP-x/SCP-2 knockout mice showed abnormal oxidation of both branched-chain fatty acid (phytanic acid) and cholesterol (cholestanoic acid) (60). However, the interpretation of results with the SCP-x/SCP-2 double knockout mice is problematic in that *i*) two proteins (i.e., SCP-x and SCP-2), rather than just SCP-x, are simultaneously ablated; *ii*) an active truncate of the SCP-x protein may be present (12); and *iii*) the L-FABP is concomitantly upregulated by 4-fold (60). The latter result is particularly relevant given that L-FABP enhances fatty acid uptake in intact cells (54, 56, 61–63), functions as a fatty acid donor for both peroxisomal and mitochondrial fatty acid oxidation in vitro (64), and binds phytanic acid, a PPARα ligand that simultaneously induces the expression of L-FABP and peroxisomal fatty acid oxidation (44, 65). L-FABP also binds other branched-chain lipids such as cholesterol (66, 67) and transports cholesterol in transfected cells (40) and liver hepatocytes (68). Thus, it is unclear whether the abnormal phytanic acid oxidation in SCP-x/SCP-2 gene-ablated mice is attributable to the absence of SCP-x, the presence of a truncated SCP-x protein, or the upregulation of L-FABP (60).

The greater effects of phytol in female compared with male mice were also reflected in liver and serum lipid profiles. Phytol-fed females exhibited decreased lipid accumulation in liver compared with phytol-fed males. Electron microscopy showed that although both male and female phytol-fed mice had fewer lipid droplets than control-fed mice, substantially less was present in phytol-fed females. Consistent with this observation, livers of phytol-fed female mice had lower total neutral lipid and lower triacylglyceride levels. However, liver cholesteryl ester levels were unaltered in phytol-fed males and increased in phytol-fed females. Serum total lipid, total neutral lipid, and cholesteryl ester levels were reduced in phytol-fed females but not males. Serum triglycerides were reduced similarly in both females and males fed phytol. These data demonstrated that the hypolipidemic effect of a dietary peroxisome proliferator (i.e., phytol) was much more pronounced in female compared with male mice.

Hypotriglyceridemic effects of branched-chain fatty acids and other compounds such as fibrates were recently reviewed by Bremer (43). Briefly, the addition of phytanic acid (or fibrates such as clofibric acid) to the diet leads to the activation of the nuclear hormone receptor PPARα, resulting in the induction of several enzymes responsible for metabolizing fatty acids, including mitochondrial and peroxisomal β-oxidation enzymes. Fatty acids in the liver are oxidized at an increased rate, decreasing the fatty acid pool, leading to reduced VLDL formation and, ultimately, decreased triglyceride content. When mice fed phytol (a branched-chain lipid) and clofibric acid (the metabolically active form of clofibrate) were compared over several parameters (liver weight, triglyceride level, and the ability to stimulate the expression of several proteins associated with fatty acid oxidation, such as L-FABP, SCP-2, and SCP-x), similar results were observed as with other peroxisomal proliferators. Liver weights were significantly increased in the both the phytol- and clofibric acid-fed mice as a result of proliferative effects. A hypotriglyceridemic effect was also observed in which levels of triglycerides decreased. In addition, hepatic levels of the cytosolic L-FABP, along with SCP-2, increased on both diets, suggesting that upregulation was mediated in response to the activation of PPARα.

The decreased serum and liver lipid levels exhibited by phytol-fed female mice compared with males was consistent with their reduced ability to metabolize phytol metabolites. Analysis by gas chromatography and mass spectrometry showed that livers and serum of phytol-fed females accumulated greatly increased levels of phytanic acid, pristanic acid, and Δ-2,3-pristanic acid compared with phytol-fed males. Levels of other downstream metabolites (i.e., 3-OH-pristanoic acid and 3-ketopristanoic acid) were unaltered and undetectable, respectively, by mass spectrometry. A similar pattern of phytol metabolite accumulation was exhibited by phytol-fed SCP-x/SCP-2 gene-ablated mice (12). Because the level of SCP-2 expression was not decreased in phytol-fed wild-type female mice, the decreased ability of females to metabolize phytol was in good agreement with *i*) female mice having substantially lower hepatic SCP-x levels (5-fold decrease) and thus less ability to metabolize phytol, and *ii*) SCP-x being the only known 3-ketoacyl-CoA thiolase that catalyzes the thiolytic cleavage of branched-chain phytol intermediates (e.g., 3-ketopristanoyl-CoA) (17). Thus, the hepatotoxicity in phytol-fed female mice was consistent with less ability to metabolize branched-chain intermediates, as shown by the accumulation of phytol metabolites upstream of the thiolytic step mediated by SCP-x.

In summary, the data presented here for the first time directly examined the in vivo effects of intrinsically lower SCP-x expression in female versus male mice on the metabolism of the branched-chain lipid phytanic acid. Although a role for SCP-x in branched-chain lipid metabolism had been postulated earlier (17), the present work shows for the first time that decreased levels of SCP-x in females correlated with the accumulation of the phytol metabolites phytanic acid, pristanic acid, and Δ-2,3-pristanic acid. Less ability to metabolize these intermediates resulted in toxicity, reflected by decreased body weight

and fat, gross liver lesions, and extensive histopathological lesions in livers of phytol-fed female mice. Male mice were not similarly affected. In addition, in the presence of phytol, protein levels of SCP-x and SCP-2 were upregulated in parallel with catalase and L-FABP, suggesting regulation by the nuclear hormone receptor PPARα. Taken together, these data were consistent with a significant role for SCP-x in the in vivo metabolism of branched-chain lipid intermediates.

REFERENCES

1. Steinberg, D., J. Avigan, C. Mize, J. H. Baxter, J. Cammermeyer, H. M. Fales, and P. F. Highet. 1966. Effects of dietary phytol and phytanic acid in animals. *J. Lipid Res.* **7:** 684–691.

2. Steinberg, D. 1983. Phytanic acid storage disease (Refsum's disease). *In* The Metabolic Basis of Inherited Disease. J. B. Stanbury, J. B. Wyngaarden, D. S. Fredrickson, J. L. Goldstein, and M. S. Brown, editors. McGraw-Hill, New York. 731–747.

3. Dietschy, J. M., and J. D. Wilson. 1970. Regulation of cholesterol metabolism. *N. Engl. J. Med.* **282:** 1128–1249.

4. Dietschy, J. M., and S. D. Turley. 2002. Control of cholesterol turnover in the mouse. *J. Biol. Chem.* **277:** 3801–3804.

5. Brown, M. S., and J. L. Goldstein. 1986. A receptor-mediated pathway for cholesterol homeostasis. *Science.* **232:** 34–47.

6. Fielding, C. J., and P. E. Fielding. 1995. Molecular physiology of reverse cholesterol transport. *J. Lipid Res.* **36:** 211–228.

7. Fielding, C. J., and P. E. Fielding. 1997. Intracellular cholesterol transport. *J. Lipid Res.* **38:** 1503–1521.

8. Avigan, J. 1966. The presence of phytanic acid in normal human and animal plasma. *Biochim. Biophys. Acta.* **166:** 391–394.

9. Verhoeven, N. M., R. J. A. Wanders, B. T. Poll-The, J. M. Saudubray, and C. Jakobs. 1998. The metabolism of phytanic acid and pristanic acid in man: a review. *J. Inherited Metab. Dis.* **21:** 697–728.

10. Pahan, K., and I. Singh. 1995. Phytanic acid oxidation: topographical localization of phytanoyl-CoA ligase and transport of phytanic acid into human peroxisomes. *J. Lipid Res.* **36:** 986–997.

11. Watkins, P. A., A. E. Howard, and S. J. Mihalik. 1994. Phytanic acid must be activated to phytanoyl-CoA prior to its alpha-oxidation in rat liver peroxisomes. *Biochim. Biophys. Acta.* **1214:** 288–294.

12. Seedorf, U., M. Raabe, P. Ellinghaus, F. Kannenberg, M. Fobker, T. Engel, S. Denis, F. Wouters, K. W. A. Wirtz, R. J. A. Wanders, N. Maeda, and G. Assmann. 1998. Defective peroxisomal catabolism of branched fatty acyl coenzyme A in mice lacking the sterol carrier protein-2/sterol carrier protein-x gene function. *Genes Dev.* **12:** 1189–1201.

13. Gallegos, A. M., B. P. Atshaves, S. M. Storey, O. Starodub, A. D. Petrescu, H. Huang, A. McIntosh, G. Martin, H. Chao, A. B. Kier, and F. Schroeder. 2001. Gene structure, intracellular localization, and functional roles of sterol carrier protein-2. *Prog. Lipid Res.* **40:** 498–563.

14. Schroeder, F., A. M. Gallegos, B. P. Atshaves, S. M. Storey, A. McIntosh, A. D. Petrescu, H. Huang, O. Starodub, H. Chao, H. Yang, A. Frolov, and A. B. Kier. 2001. Recent advances in membrane cholesterol microdomains: rafts, caveolae, and intracellular cholesterol trafficking. *Exp. Biol. Med.* **226:** 873–890.

15. Schroeder, F., A. Frolov, J. Schoer, A. Gallegos, B. P. Atshaves, N. J. Stolowich, A. I. Scott, and A. B. Kier. 1998. Intracellular cholesterol binding proteins, cholesterol transport and membrane domains. *In* Intracellular Cholesterol Trafficking. T. Y. Chang and D. A. Freeman, editors. Kluwer Academic Publishers, Boston. 213–234.

16. Seedorf, U., P. Brysch, T. Engel, K. Schrage, and G. Assmann. 1994. Sterol carrier protein X is peroxisomal 3-oxoacyl coenzyme A thiolase with intrinsic sterol carrier and lipid transfer activity. *J. Biol. Chem.* **269:** 21277–21283.

17. Wanders, R. J., E. van Berkel, F. Wouters, K. W. A. Wirtz, and U. Seedorf. 1998. Identification of the newly discovered 58 kDa peroxisomal thiolase SCP-x as the main thiolase involved in both pristanic acid and trihydroxycholestanoic acid oxidation: implications for peroxisomal beta-oxidation disorders. *J. Inherited Metab. Dis.* **21:** 302–305.

18. Bun-ya, M., M. Maebuchi, T. Kamiryo, T. Kurosawa, M. Sato, M. Tohma, L. L. Jiang, and T. Hashimoto. 1998. Thiolase involved in bile acid formation. *J. Biochem.* **123:** 347–352.

19. Wanders, R. J., S. Denis, F. Wouters, K. W. A. Wirtz, and U. Seedorf. 1997. Sterol carrier protein X (SCPx) is a peroxisomal branched-chain beta-ketothiolase specifically reacting with 3-oxo-pristanoyl-CoA: a new, unique role for SCPx in branched-chain fatty acid metabolism in peroxisomes. *Biochem. Biophys. Res. Commun.* **236:** 565–569.

20. Schroeder, F., and G. Nemecz. 1989. Interaction of sphingomyelins and phosphatidylcholines with fluorescent dehydroergosterol. *Biochemistry.* **28:** 5992–6000.

21. Ferdinandusse, S., S. Denis, E. van Berkel, G. Dacremont, and R. J. Wanders. 2000. Peroxisomal fatty acid oxidation disorders and 58 kDa sterol carrier protein X (SCPx): activity measurements in liver and fibroblasts using a newly developed method. *J. Lipid Res.* **41:** 336–342.

22. Muench, C., A. Hafer, N. Katzberg, J. Scheibner, E. F. Stange, U. Seedorf, and M. Fuchs. 2000. Relevance of the sterol carrier protein-2 gene for bile acid synthesis and gallstone formation in genetically susceptible mice (Abstract). *Gastroenterology.* **118 (Suppl. 2):** 1167.

23. Schroeder, F., S. C. Myers-Payne, J. T. Billheimer, and W. G. Wood. 1995. Probing the ligand binding sites of fatty acid and sterol carrier proteins: effects of ethanol. *Biochemistry.* **34:** 11919–11927.

24. Frolov, A., T. H. Cho, J. T. Billheimer, and F. Schroeder. 1996. Sterol carrier protein-2, a new fatty acyl coenzyme A-binding protein. *J. Biol. Chem.* **271:** 31878–31884.

25. Colles, S. M., J. K. Woodford, D. Moncecchi, S. C. Myers-Payne, L. R. McLean, J. T. Billheimer, and F. Schroeder. 1995. Cholesterol interactions with recombinant human sterol carrier protein-2. *Lipids.* **30:** 795–804.

26. Murphy, E. J. 1998. Sterol carrier protein-2 expression increases fatty acid uptake and cytoplasmic diffusion in L-cell fibroblasts. *Am. J. Physiol.* **275:** G237–G243.

27. McArthur, M. J., B. P. Atshaves, A. Frolov, W. D. Foxworth, A. B. Kier, and F. Schroeder. 1999. Cellular uptake and intracellular trafficking of long chain fatty acids. *J. Lipid Res.* **40:** 1371–1383.

28. Atshaves, B. P., S. M. Storey, and F. Schroeder. 2003. Sterol carrier protein-2/sterol carrier protein-x expression differentially alters fatty acid metabolism in L cell fibroblasts. *J. Lipid Res.* **44:** 1751–1762.

29. Atshaves, B. P., S. M. Storey, A. D. Petrescu, C. C. Greenberg, O. I. Lyuksyutova, R. Smith, and F. Schroeder. 2002. Expression of fatty acid binding proteins inhibits lipid accumulation and alters toxicity in L-cell fibroblasts. *Am. J. Physiol.* **283:** C688–C703.

30. Roff, C. F., A. Pastuszyn, J. F. I. Strauss, J. T. Billheimer, M. T. Vanier, R. O. Brady, T. J. Scallen, and P. G. Pentchev. 1992. Deficiencies in sex-regulated expression and levels of two hepatic sterol carrier proteins in a murine model of Niemann-Pick type C disease. *J. Biol. Chem.* **267:** 15902–15908.

31. Atshaves, B. P., A. Petrescu, O. Starodub, J. Roths, A. B. Kier, and F. Schroeder. 1999. Expression and intracellular processing of the 58 kDa sterol carrier protein 2/3-oxoacyl-CoA thiolase in transfected mouse L-cell fibroblasts. *J. Lipid Res.* **40:** 610–622.

32. Thigpen, J. E., K. D. R. Setchell, K. B. Ahlmark, J. Locklear, T. Spahr, G. F. Caviness, M. F. Goelz, J. K. Haseman, R. R. Newbold, and D. B. Forsythe. 1999. Phytoestrogen content of purified, open- and closed-formula laboratory animal diets. *Lab. Anim. Sci.* **49:** 530–536.

33. Thigpen, J. E., K. D. R. Setchell, M. F. Goelz, and D. B. Forsythe. 1999. The phytoestrogen content of rodent diets (Abstract). *Environ. Health Perspect.* **107:** A182–A183.

34. Van den Branden, C., J. Vamecq, I. Wybo, and F. Roels. 1986. Phytol and peroxisome proliferation (Abstract). *Pediatr. Res.* **20:** 411–415.

35. Nagy, T. R., and A-L. Clair. 2000. Precision and accuracy of dual-

energy X-ray absorptiometry for in vivo body composition in mice. *Obes. Res.* **8:** 392–398.

36. Hall, P. F., B. M. Gormley, L. R. Jarvis, and R. D. Smith. 1980. A staining method for the detection and measurement of fat droplets in hepatic tissue. *Pathology.* **12:** 605–608.

37. Kopp-Schneider, A. 2003. Biostatistical evaluation of focal hepatic preneoplasia. *Toxicol. Pathol.* **31:** 121–125.

38. Puglielli, L., A. Rigotti, L. Amigo, L. Nunez, A. V. Greco, M. J. Santos, and F. Nervi. 1996. Modulation of intrahepatic cholesterol trafficking: evidence by *in vivo* antisense treatment for the involvement of sterol carrier protein-2 in newly synthesized cholesterol transfer into bile. *Biochem. J.* **317:** 681–687.

39. Hara, A., and N. S. Radin. 1978. Lipid extraction of tissues with a low toxicity solvent. *Anal. Biochem.* **90:** 420–426.

40. Jefferson, J. R., J. P. Slotte, G. Nemecz, A. Pastuszyn, T. J. Scallen, and F. Schroeder. 1991. Intracellular sterol distribution in transfected mouse L-cell fibroblasts expressing rat liver fatty acid binding protein. *J. Biol. Chem.* **266:** 5486–5496.

41. Marzo, A., P. Ghirardi, D. Sardini, and G. Meroni. 1971. Simplified measurement of monoglycerides, diglycerides, triglycerides, and free fatty acids in biological samples. *Clin. Chem.* **17:** 145–147.

42. Bradford, M. 1976. A rapid and sensitive method for the quantitation of microgram quantities of protein utilizing the principle of protein-dye binding. *Anal. Biochem.* **72:** 248–254.

43. Bremer, J. 2001. The biochemistry of hypo- and hyperlipidemic fatty acid derivatives: metabolism and metabolic effects. *Prog. Lipid Res.* **40:** 231–268.

44. Wolfrum, C., P. Ellinghaus, M. Fobker, U. Seedorf, G. Assmann, T. Borchers, and F. Spener. 1999. Phytanic acid is ligand and transcriptional activator of murine liver fatty acid binding protein. *J. Lipid Res.* **40:** 708–714.

45. Ellinghaus, P., C. Wolfrum, G. Assmann, F. Spener, and U. Seedorf. 1999. Phytanic acid activates the peroxisome proliferator-activated receptor alpha (PPARalpha) in sterol carrier protein-2-/sterol carrier protein-x-deficient mice. *J. Biol. Chem.* **274:** 2766–2772.

46. Gordon, G. B. 1977. Saturated free fatty acid toxicity. II. Lipid accumulation, ultrastructural alterations, and toxicity in mammalian cells in culture. *Exp. Mol. Pathol.* **27:** 262–276.

47. Gordon, G. B. 1978. Saturated free fatty acid toxicity. III. Potentiation by chlorophenoxyisobutyrate (clofibrate) in strain L cells. *Res. Commun. Chem. Pathol. Pharmacol.* **20:** 79–99.

48. Stolowich, N. J., A. Frolov, B. P. Atshaves, E. Murphy, C. A. Jolly, J. T. Billheimer, A. I. Scott, and F. Schroeder. 1997. The sterol carrier protein-2 fatty acid binding site: an NMR, circular dichroic, and fluorescence spectroscopic determination. *Biochemistry.* **36:** 1719–1729.

49. McLean, M. P., J. T. Billheimer, K. J. Warden, and R. B. Irby. 1995. Differential expression of hepatic sterol carrier proteins in the streptozotocin-treated diabetic rat. *Endocrinology.* **136:** 3360–3368.

50. McLean, M. P., Z. Zhao, and G. C. Ness. 1995. Reduced hepatic LDL-receptor, 3-hydroxy-3-methylglutaryl CoA reductase and sterol carrier protein-2 is associated with pregnancy loss in the diabetic rat. *Endocrine.* **3:** 695–703.

51. Ohba, T., J. A. Holt, J. T. Billheimer, and J. F. I. Strauss. 1995. Human sterol carrier protein x/sterol carrier protein 2 gene has two promoters. *Biochemistry.* **34:** 10660–10668.

52. Seedorf, U., U. Raabe, and G. Assmann. 1993. Cloning, expression and sequence of SCP-X encoding cDNAs and a related pseudogene. *Gene.* **123:** 165–172.

53. Bonen, A., J. J. F. P. Luiken, S. Liu, D. J. Dyck, B. Kiens, S. Kristiansen, L. P. Turcotte, G. J. Van der Vusse, and J. F. Glatz. 1998. Palmitate transport and fatty acid transporters in red and white muscles. *Am. J. Physiol.* **275:** E471–E478.

54. Murphy, E. J., D. R. Prows, J. R. Jefferson, and F. Schroeder. 1996. Liver fatty acid binding protein expression in transfected fibroblasts stimulates fatty acid uptake and metabolism. *Biochim. Biophys. Acta.* **1301:** 191–198.

55. Murphy, E. J., D. R. Prows, J. R. Jefferson, S. Incerpi, Z. I. Hertelendy, C. E. Heiliger, and F. Schroeder. 1996. Cis-parinaric acid uptake in L-cells. *Arch. Biochem. Biophys.* **335:** 267–272.

56. Murphy, E. J. 1998. L-FABP and I-FABP expression increase NBD-stearate uptake and cytoplasmic diffusion in L-cells. *Am. J. Physiol.* **38:** G244–G249.

57. Atshaves, B. P., S. Storey, H. Huang, and F. Schroeder. 2004. Liver fatty acid binding protein expression enhances branched-chain fatty acid metabolism. *Mol. Cell. Biochem.* In press.

58. Costet, P., C. Legendre, J. More, A. Edgar, P. Galtier, and T. Pineau. 1998. PPARalpha deficiency leads to progressive dyslipidemia with sexually dimorphic obesity and steatosis. *J. Biol. Chem.* **273:** 29577–29585.

59. Shimano, H., J. D. Horton, R. E. Hammer, I. Shimomura, M. S. Brown, and J. L. Goldstein. 1996. Overproduction of cholesterol and fatty acids causes massive liver enlargement in transgenic mice expressing truncated SREBP-1a [see comments]. *J. Clin. Invest.* **98:** 1575–1584.

60. Seedorf, U. 1998. Functional analysis of sterol carrier protein-2 (SCP2) in SCP2 knockout mouse. *In* Intracellular Cholesterol Trafficking. T. Y. Chang and D. A. Freeman, editors. Kluwer Academic Publishers, Boston. 233–252.

61. Prows, D. R., E. J. Murphy, and F. Schroeder. 1995. Intestinal and liver fatty acid binding proteins differentially affect fatty acid uptake and esterification in L-cells. *Lipids.* **30:** 907–910.

62. Luxon, B. A., and R. A. Weisiger. 1993. Sex differences in intracellular fatty acid transport: role of cytoplasmic binding proteins. *Am. J. Physiol.* **265:** G831–G841.

63. Weisiger, R. A. 1996. Cytoplasmic transport of lipids: role of binding proteins. *Comp. Biochem. Physiol.* **115B:** 319–331.

64. Reubsaet, F. A., J. H. Veerkamp, M. L. Bruckwilder, J. M. Trijbels, and L. A. Monnens. 1990. The involvement of fatty acid-binding protein in peroxisomal fatty acid oxidation. *FEBS Lett.* **267:** 229–230.

65. Frolov, A., K. Miller, J. T. Billheimer, T-C. Cho, and F. Schroeder. 1997. Lipid specificity and location of the sterol carrier protein-2 fatty acid binding site: a fluorescence displacement and energy transfer study. *Lipids.* **32:** 1201–1209.

66. Schroeder, F., M. E. Dempsey, and R. T. Fischer. 1985. Sterol and squalene carrier protein interactions with fluorescent delta 5,7,9(11)-cholestatrien-3 beta-ol. *J. Biol. Chem.* **260:** 2904–2911.

67. Schroeder, F., P. Butko, G. Nemecz, J. R. Jefferson, D. Powell, Z. Rymaszewski, M. E. Dempsey, J. Kukowska-Latallo, and J. B. Lowe. 1989. Sterol carrier protein: a ubiquitous protein in search of a function. *In* Bioengineered Molecules: Basic and Clinical Aspects. R. Verna, R. Blumenthal, and L. Frati, editors. Raven Press, New York. 29–45.

68. Fuchs, M., A. Hafer, C. Muench, F. Kannenberg, S. Teichmann, J. Scheibner, E. F. Stange, and U. Seedorf. 2001. Disruption of the sterol carrier protein 2 gene in mice impairs biliary lipid and hepatic cholesterol metabolism. *J. Biol. Chem.* **276:** 48058–48065.